JOURNAL OF GUIDANCE, CONTROL, AND DYNAMICS
Vol. 20, No. 6, November–December 1997

von Kármán Lecture

Adventures on the Interface of Dynamics and Control

John L. Junkins
Texas A&M University, College Station, Texas 77843-3141

Controllers for dynamic systems are best designed, on the average, by analysts whose expertise encompasses both modeling of the class of systems under discussion and methodology for designing controllers. Good decisions on issues such as selection of coordinates, modeling approximations, selection/design and location of sensors and actuators, and definition of meaningful performance measures require expertise beyond algebraic/computational methods for control design. This commonsense viewpoint underlies a significant trend toward a unified development of analysis methodology for mechanics and control, especially with regard to spacecraft dynamics, stability, estimation, and control. This paper overviews recent developments and discusses several "adventures" that illustrate mechanics-based insights useful in modern applications. The discussion spans orbital dynamics, attitude dynamics and control, and nonlinear multibody dynamics and control and considers both conceptual developments and results from several successful missions.

I. Introduction

DYNAMICS and control analysis and associated design methods have matured rapidly over the past three decades. In spite of significant advances, however, developing reliable and well-optimized controllers for aerospace vehicles remains an iterative and labor-intensive art form. This is because the increasing size, structural flexibility, and dynamic complexity, coupled with competing demands for greater precision and autonomy, continue to outstrip our ability to model these systems adequately. A second set of difficulties complicate practical applications: the traditional discipline specializations result in few engineers having sufficient breadth and depth of expertise to resolve efficiently problems involving coupling between mechanics, controls, electro-mechanics, electro-optics, and computer subsystems.

It is evident that crucial issues lie on the interface of traditional disciplines. These are difficult to resolve efficiently because of the implicitly required coupled effort of a group of engineers. Responding to these challenges, engineers with increased breadth and depth have emerged over the past two decades. Researchers working on the mechanics and controls interface have published hundreds of papers (see the survey by Hyland et al.[1]) and several texts[2–7]; these document the multidisciplinary arena: mechanics and control of dynamic systems.

In analysis of nonlinear mechanical systems, a set of fundamental modeling issues surrounds the choice of coordinates used to describe the system dynamics. These decisions impact design and synthesis of controllers because a given physical system may be described rigorously by sets of regular, near-linear differential equations or, equivalently, in the Lagrangian generalized coordinates sense, by highly nonlinear equations containing singularities, with the "degree of nonlinearity" depending strongly on the coordinates selected. Much of the early history of dynamics addressed the quest for judicious coordinates under natural forces like gravity (consider the field of celestial mechanics).

A. Coordinate Transformation Issues

Classic coordinate transformation methodology, e.g., Hamilton's canonical transformation theory and Hamilton–Jacobi theory,[8] focus on finding ignorable coordinates and analytical integrals of the motion, rather than finding coordinates governed by the most nearly linear differential equations over a state-space domain of interest. These methodologies were developed for open-loop initial and/or two-point boundary value problems considering (typically) conservative systems. These remarks are most easily understood when one considers the classic Lagrangian viewpoint where coordinates define the location of all mass in the system, i.e., the system's geometric configuration. Another level of transformation generality was established by Hamilton; his phase space coordinates are essentially the canonical version of modern state variables. In this view of state-space analysis, coordinates define both position (geometric configuration) and velocity (or momentum), and coordinate transformation implies a contact transformation operation where one set of position/velocity state-space coordinates are nonlinearly mapped into another.[8]

John L. Junkins received his M.S. and Ph.D. from the University of California, Los Angeles, in 1967 and 1969, respectively, and his B.A.E. from Auburn University in 1965. He has held the George Eppright Endowed Chair Professorship at Texas A&M University since 1985. He is Founding Director, Center for Mechanics and Control (1991–present). Previous academic appointments were at the University of Virginia (1970–1977) and Virginia Polytechnic Institute and State University (1978–1985). He has held positions at McDonnell Douglas Astronautics Company (1965–1970) and NASA Marshall Space Flight Center (1962–1965). Dr. Junkins' interests include navigation, guidance, and control; celestial mechanics; dynamical systems; optimization; structural mechanics/controls; and sensing/actuation. His ideas have been implemented in over a dozen major aerospace and industrial systems. He researches analytical, computational, and experimental methods, and he consults widely on applications. He is a member of the National Academy of Engineering and the International Academy of Astronautics; he is a Fellow of the AIAA and the American Astronautical Society (AAS). He has received 10 national or international honors, including the 1983 AIAA Mechanics and Control of Flight Award, the 1987 AAS Dirk Brouwer Award, the 1988 AIAA John Leland Atwood Award, the 1990 AIAA Pendray Aerospace Literature Award, and the 1997 Theodore von Kármán Lectureship in Astronautics. He has directed the research of over 50 graduate students and 10 postdoctoral researchers. Dr. Junkins has over 330 publications, including three authored texts, three edited texts, one patent, and over 100 archival journal publications.

Received Nov. 6, 1996; presented as Paper 97-0002 at the AIAA 35th Aerospace Sciences Meeting, Reno, NV, Jan. 6–9, 1997; revision received March 11, 1997; accepted for publication March 11, 1997.

Feedback linearization considers an additional level of generality, simultaneously transforming position, velocity, and control variables. The idea is to absorb all nonlinear terms in a given differential equation model into judicious nonlinear state transformations and feedback laws. Important early work includes that of Krener,[9] Hermann and Krener,[10] Brockett,[11] Jakubczyk and Respondek,[12] Hunt and Su,[13] Junkins et al.,[14] Hunt et al.,[15] and Isidori et al.[16] Excellent introductory treatments are given by Isidori,[17] Nijmeijer and van der Schaft,[18] and Slotine and Li.[19] For certain problems, we can establish asymptotic stability, disturbance decoupling, noninteracting control, and output regulation. These transformations are generally exact, i.e., not Taylor's series. In some cases, the transformations can be found by inspection by simply specifying part of the controls to cancel all nonlinear terms appearing in the equations of motion, and the remaining part of the control can be an additive linear state feedback, resulting in a linear closed-loop system. Thus, the linear control is mapped back through the inverse nonlinear transformation to generate actuator commands.

Feedback linearizing transformations can be obtained as the solution of a set of coupled partial differential equations. Assuming that a solution can be obtained, the major practical problem is that exact cancellation of the nonlinearities requires perfect knowledge of the system dynamics. Cancellation is not exact in applications and the resulting feedback linearized input–output behavior may be a poor approximation of the actual system's behavior. In the worst cases, instability may result. One approach to enhance robustness is to apply adaptive techniques to achieve asymptotic behavior in the presence of model uncertainties, e.g., see Refs. 20–24. Estimation-based adaptive schemes have been proposed by Pomet and Praly,[25] Compion and Bastin,[26] Han et al.,[27] and Teel et al.[28] Another practical consideration is that, in many instances, canceling nonlinearities is neither necessary nor desirable. For example, it can be shown[29–33] that the general nonlinear dynamics of a tumbling asymmetric satellite can be globally stabilized by several different linear feedback control laws, and this can be done without the necessity of introducing the possible loss of robustness through feedback linearization.

An interesting application of feedback linearization is attitude control and momentum management of a spacecraft in low-Earth orbit, e.g., consider the international space station (ISS) project. The difficulty lies in keeping the spacecraft in an Earth-pointing attitude by using momentum exchange actuators for control while desaturating the same actuators working against gravity gradient torques. The problem is amenable to feedback linearization (cf. Refs. 34–36). Other related works include those by Singh and Iyer[37] and Singh and Bossart.[38] An easily appreciated source of uncertainty in the ISS attitude control and momentum management problem lies in poor knowledge of the inertia matrix. Conceptually, it is possible to predict the inertia matrix as a function of the locations and motions of the ISS components. However, rather than attempting to model to high precision the 30-year evolution of the ISS, it seems more sensible to design a robust controller that guarantees stablility for a wide range of mass properties. Sheen and Bishop[35] applied direct adaptive methods; the ISS attitude and control moment gyro momentum were controlled with large uncertainties in the inertias and attitude errors outside the linear range. The indirect adaptive approach embodies a distinct parameter identification module. Paynter and Bishop[39] show that Kalman filter parameter identification with feedback linearization control compares favorably with direct adaptive control. A model reference adaptive control method that accommodates unknown inertias and that guarantees asymptotic stability for a class of nonlinear attitude control problems was introduced by Junkins et al.[32]

B. Overview of Spacecraft Attitude Maneuvers

Attitude maneuvers represent an interesting class of nonlinear spacecraft control problems where theory, computation, ground experiment, and on-orbit implementation have converged over the past two decades. It is an area where spacecraft dynamics plays a particularly important role in obtaining the necessary insights to achieve useful results from application of stability and control theory. These problems inherently suffer from the triple curse of nonlinearity, high dimensionality, and model errors. Furthermore,

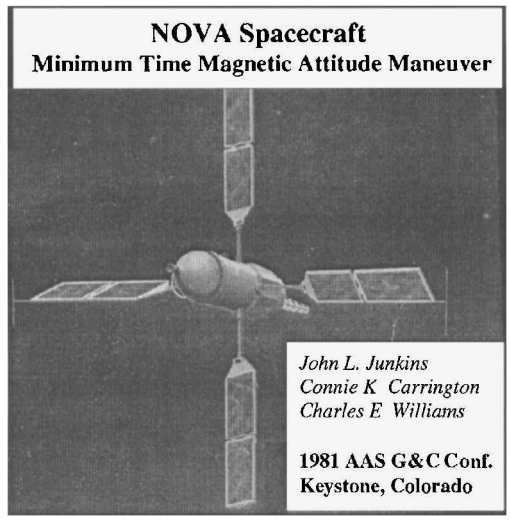

Fig. 1 NOVA navy navigation satellite.

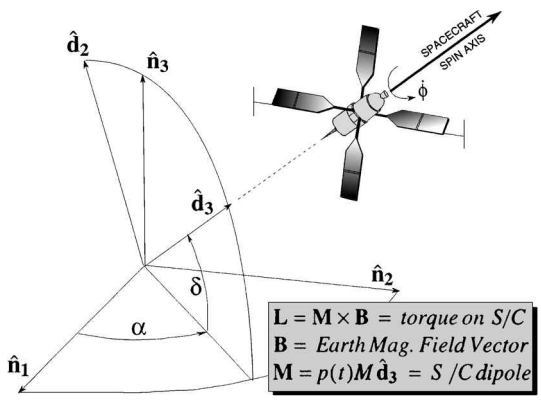

Fig. 2 Orientation of the NOVA spin axis.

application of optimal control is difficult because often no single performance measure can capture the mission objectives. For example, minimum time, minimum energy, minimum sensitivity to errors, and minimum vibration are inherently competitive performance measures. Important recent literature on this class of problems are the works by Wie, Junkins, Schaub, Mukherjee, Robinett, and colleagues.[3,4,6,29,30,40–47] Section IV of this paper considers recent developments and mission results.

The first on-orbit implementation of an optimal control derived from Pontryagin's Principle was the 1981 minimum-time magnetic-attitude maneuvers for the NOVA family of navigation spacecraft[6,40] depicted in Figs. 1 and 2. The NOVA vehicle spins at ~5 rpm and an electromagnet aligned with the spin axis interacts with the Earth's magnetic field to generate a torque transverse to the spin axis and precess the spacecraft slowly. The polarity of the electromagnet is the control variable and the problem is easily stated: given the spacecraft spin axis pointing direction (α_0, δ_0) = initial right ascension and declination at time t_0, determine the polarity history $-1 \leq p(t) \leq 1$ required to achieve a minimum-time reorientation of the spin axis to a desired target state (α_T, δ_T). A direct assault on this problem with Pontryagin's principle[6] leads to a twelfth-order nonlinear two-point boundary value problem that is not compatible with near-real-time implementation. However, it has been shown that use of a passive damper reduces nutation quickly compared to a slow precession of the angular-momentum vector.[40] This observation permits a two-timescale approximation and results in a dramatic order reduction to a fourth-order system. The optimum control is generated as a nonlinear bang-bang controller with multiple polarity $[p(t) = \pm 1]$ switches determined as the sign of a nonlinear switching function. Solving the two-point boundary value problem is reduced to finding a single unknown $0 \leq \gamma_0 \leq 360$ deg that generates the entire family of extremal trajectories. We use a special inertial frame with (right ascension, declination) = (α^*, δ^*) defined so that

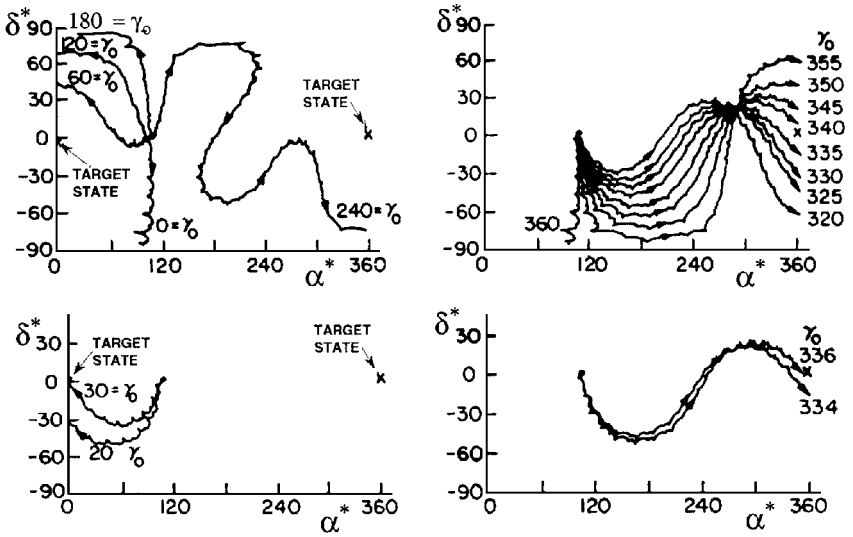

Fig. 3 Extremal field map of minimum time maneuvers.

the initial state is on the equator and the target state is the origin; this simplifies the solution of the two-point boundary problem. In fact it is reduced to a "video game" interface where the graphic solution is obtained in several "screens" as illustrated in Fig. 3. Note that the solution is obtained by sweeping γ_0 at some interval $\Delta\gamma_0$ between chosen limits and graphically observing the γ_0 region where the trajectory passes nearest the origin. It is easy to isolate the origin to within a fraction of a degree within three or four screens; this is the procedure implemented successfully for the NOVA missions. In Fig. 3, it is evident that there are two local solutions; this is because one can travel south from San Francisco to Los Angeles, but one can also traverse the great circle "the long way" and pass over the North Pole, if persistent! The cusps are polarity reversal points where the direction of precession reverses. The maneuver shown for $\gamma_0 \sim 30$ deg required 19 switches and more than 7 h to reorient the pointing direction from ($\alpha_0 = 45.2$ deg, $\delta_0 = 35.1$ deg) to ($\alpha_T = -42.7$ deg, $\delta_T = -31.4$ deg).

This elegant application of optimal control theory was formulated just a few months before the launch of the first NOVA spacecraft in May 1981 and represents an excellent example of the synergy between dynamics and controls. It replaced a nonlinear programming approach (iterating a nonlinear attitude simulation searching on 10–30 unknown switch times) that did not converge reliably and was not compatible with real-time mission support. This approach replaces this nonlinear programming approach to switch time optimization with the bounded one-dimensional search. For this mission, given attitude determination information at the beginning of a 10-min pass of the satellite over the Laurel, Maryland, Johns Hopkins Applied Physics Laboratory's mission control center, this algorithm could be executed in about 5 min of real time and uploaded to the spacecraft computer while it was still above the horizon for implementation over the next few hours. In the actual mission, the first (>7 h) maneuver was followed by a trim maneuver of several minutes to null a final error of ~1 deg; the small residual error was due to the approximate fourth-order spherical harmonic model used for the geomagnetic field.

C. Overview of This Paper

With the preceding introduction, we turn to some more recent developments and present some results of relatively broad significance. Although the issues discussed are presented in the context of spacecraft dynamics, estimation, and control, they are developed in a way that reveals broadly useful concepts. Most of the developments address aspects of how to transform or approximate the system dynamics to advance toward solution of important problems. Coordinate choice is one major common issue; we address some aspects of this subject first.

It is obvious that an infinity of coordinates is generally possible; seeking the most nearly linear description of a given system's dynamics is an attractive philosophical point of view for coordinate transformations and/or choosing between available coordinate sets. This suggests that before resorting to feedback linearization and/or adaptive controller design for a given system, we should first seek the best coordinates vis-à-vis smallness of nonlinearities and in view of the application under consideration. A useful starting point is to develop a broadly applicable measure of the degree of nonlinearity and compute this measure for various coordinate sets to help inform these decisions. Of course, coordinate selection and transformation are but two of many issues that must be addressed in dynamics and control analysis, and, although it plays a role in each of the "adventures" discussed here, we will discuss other important mechanics-based issues for controller design in the context of particular problems.

In Sec. II, we introduce error propagation concepts and apply them to approximation of the nonlinear error analysis in orbital and attitude dynamics. Several coordinate choices and their relative merits are studied vis-à-vis the validity of linear error theory. The methodology is validated through use of the Monte Carlo method. Although the error propagation problem is used to study the validity of dynamic nonlinearity, it is evident that the methods introduced are also of relevance in finding near-linear dynamic models for control design and, more broadly, measuring the validity of linearity assumptions in particular applications.

In Sec. III, we present a recently introduced orthogonal quasicoordinate formulation for multibody dynamics. We show how to generate, by solving kinematic-like differential equations, the instantaneous spectral decomposition of a configuration variable mass matrix typical of those arising in large deformations of robot manipulators. Through this formulation, it is possible to bypass inversion of the configuration-variable mass matrix and define quasicoordinates for which the mass matrix is an identity matrix. Solving these differential equations leads to a robust simulation of nonlinear multibody system dynamics. This formulation is easy to parallelize and, therefore, is an attractive approach for high-dimensional systems.

In Sec. IV, we consider some recent research on design of globally stabilizing feedback control laws for large-angle spacecraft reorientation maneuvers. These results utilize Lyapunov stability theory in some interesting ways. To complement results from analytical and computational studies, we consider on-orbit results from the recent Clementine lunar mission.[31]

II. Nonlinear Systems Error Propagation

Figure 4 is a qualitative sketch showing how a surface of constant probability evolves during the orbit of a near-Earth spacecraft, where the motion initiates with a known Gaussian distribution of errors in initial position and velocity. It is known that these surfaces of constant probability are typically well approximated over small time intervals by ellipsoids[48]; however, over longer times, the region of uncertainty becomes banana-shaped and, eventually, wraps around

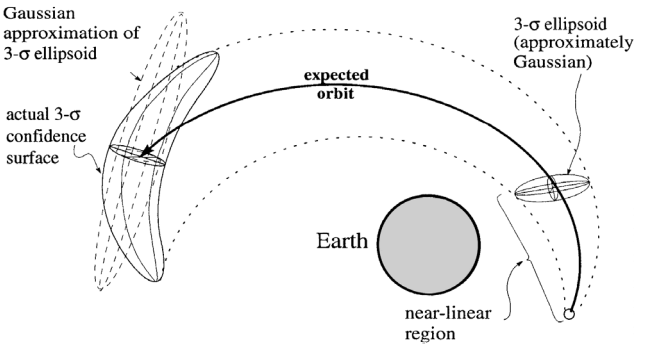

Fig. 4 Evolution of uncertainty in orbital mechanics.

the Earth in a (qualitative) toroidal tube of uncertainty. We show that the shapes of confidence-surface approximations, and therefore their validity, are strongly dependent on the coordinate choice. We also note the conceptual equivalence of propagating initial condition uncertainty of a single object to the distribution dynamics (or cloud dynamics) of particles (idealized as identical) after an explosion. Thus, the evolution of uncertainty is an approximate dual of the planetary ring formation problem.

A. Error Propagation in Orbital Mechanics

Figure 5 shows the distribution of 200 Monte Carlo positions, projected into the nominal orbit plane, at quarter-period intervals of one complete nominal orbit, where τ is time measured in fractions of the nominal unperturbed orbital period. Also shown are three analytical predictions of the 3σ confidence boundaries. Three analytical confidence predictions use linear error theory with three coordinate choices for linearization of the dynamics: 1) rectangular coordinates, 2) polar coordinates, and 3) classic orbital elements (variation of parameters method). In this study, only initial condition uncertainty is considered.

The dynamic model[48] includes perturbations by Earth oblateness (J_2) and atmospheric drag. It is obvious by inspection of Fig. 5 at $\tau = 1$ that the confidence surfaces predicted by linear error theory in polar coordinates and orbital elements are superior to the linear error theory in rectangular coordinates.

For the numerical simulations underlying Fig. 5, the following parameters for the nominal orbit are assumed. At injection, the nominal perigee altitude is 300 km, the orbit eccentricity is 0.2, the inclination of nominal orbital plane is 10 deg, the longitude of ascending node is 45 deg, and the argument of perigee is 20 deg. The mass of each sample Monte Carlo particle is taken to be 0.5 kg, with a radius of 0.17 m. The ballistic drag coefficient corresponding to the orbiting particle is taken to be equal to 1.2. The uncertainty of the initial conditions, for the purposes of generating this example, were assumed as uncorrelated zero mean Gaussian errors with the initial position error standard deviation of 2 km and the initial velocity error standard deviation of 0.002 km/s in all three components (equatorial rectangular coordinates).

To see how linear error theory can be used to approximate nonellipsoidal confidence boundaries, shown in Fig. 5, note that an ellipsoid (using linear error theory), when mapped through a nonlinear coordinate transformation, is not an ellipsoid! This idea is captured qualitatively in Fig. 6. Finding a coordinate transformation that enhances the validity of linear error theory is of great consequence, because it may allow us to bypass the expense and associated convergence difficulties of a Monte Carlo process.

B. Judicious Use of Linear Error Theory Approximations for Nonlinear Dynamic Systems

Consider a linear algebraic model of the form

$$\boldsymbol{y} = A\boldsymbol{x} + \boldsymbol{b} \tag{1}$$

where $\boldsymbol{y} \in \mathcal{R}^{m\times 1}$ and $\boldsymbol{x} \in \mathcal{R}^{n\times 1}$ are random vectors, whereas $\boldsymbol{b} \in \mathcal{R}^{m\times 1}$ and $A \in \mathcal{R}^{m\times n}$ are known constant matrices. Question: If we know the first two statistical moments of $\boldsymbol{x}$

$$\bar{\boldsymbol{x}} = E\{\boldsymbol{x}\} \qquad P_{xx} = E\{(\boldsymbol{x}-\bar{\boldsymbol{x}})(\boldsymbol{x}-\bar{\boldsymbol{x}})^T\} \tag{2}$$

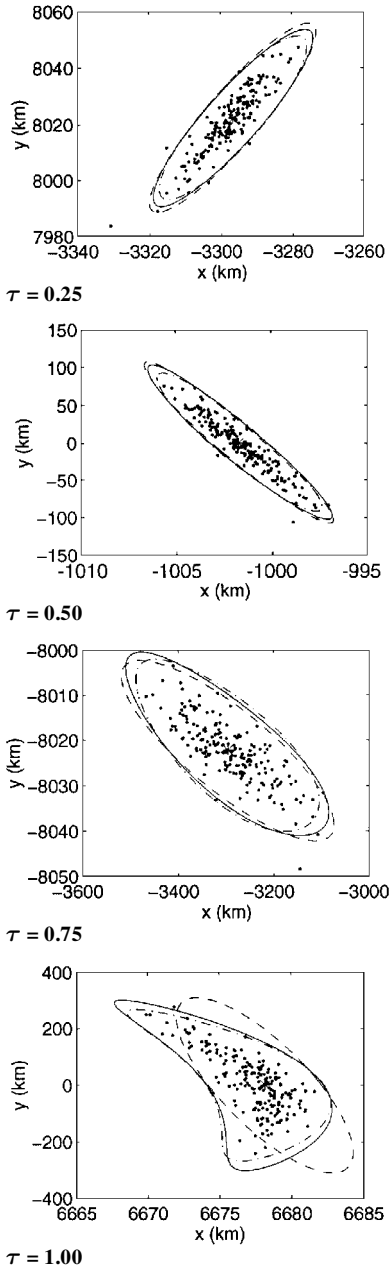

Fig. 5 Analytical estimation of 3σ confidence surfaces: 3σ surfaces computed based on linearization of the differential equations for – – –, rectangular coordinates; –·–, polar coordinates; and ——, orbit elements.

what are the corresponding statistical moments of $\boldsymbol{y}$? The answer is well known.[49] The mean and covariance moments of $\boldsymbol{y}$ are given by the mappings

$$\bar{\boldsymbol{y}} = A\bar{\boldsymbol{x}} + \boldsymbol{b} \qquad P_{yy} = AP_{xx}A^T \tag{3}$$

Furthermore, if $\boldsymbol{x} = \bar{\boldsymbol{x}} + \delta\boldsymbol{x}$ belongs to a multidimensional Gaussian probability density distribution

$$f(\boldsymbol{x}) = \frac{1}{(2\pi)^{n/2}|P_{xx}|^{\frac{1}{2}}} \exp\left\{-\frac{1}{2}\delta\boldsymbol{x}^T P_{xx}^{-1}\delta\boldsymbol{x}\right\} \tag{4}$$

then $\boldsymbol{y}$ belongs to another Gaussian distribution obtained from Eq. (4) by replacing $(x, \boldsymbol{x}, n)$ by $(y, \boldsymbol{y}, m)$ (denoted by $x \to y$). Observe that the surfaces of constant probability density are the two hyperellipsoids

$$[\boldsymbol{x}-\bar{\boldsymbol{x}}]^T P_{xx}^{-1}[\boldsymbol{x}-\bar{\boldsymbol{x}}] = r^2 \qquad x \to y \tag{5}$$

and that $r = 3$ defines the 3σ error surface. Note that the integral of the density function [Eq. (4)] over the interior of the volume bounded by Eq. (5) is the probability that $\delta\boldsymbol{x}$ is contained within the

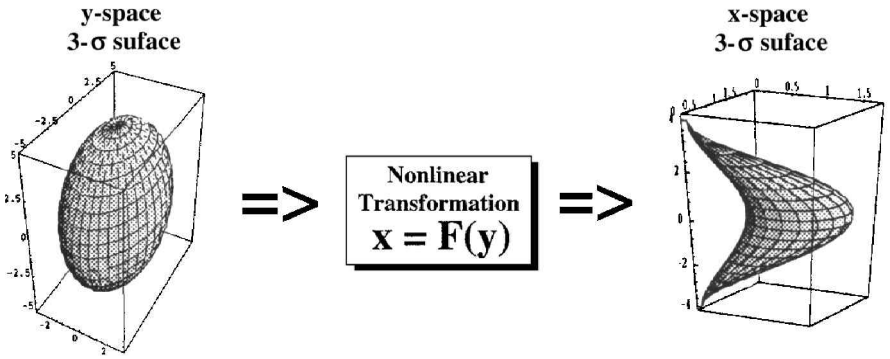

Fig. 6 Confidence surfaces mapped through nonlinear coordinate transformations.

ellipsoid of Eq. (5). For an ($n = 6$)-dimensional 3σ ellipsoid, the probability that $\delta \boldsymbol{x}^T P_{xx}^{-1} \delta \boldsymbol{x} \leq 3^2$ is ~0.9.

These results apply with some degree of approximation for nonlinear transformations in lieu of Eq. (1), where A is interpreted as a locally evaluated Jacobian: $A = \partial \boldsymbol{y}/\partial \boldsymbol{x}$ and $\delta \boldsymbol{y} \cong A \delta \boldsymbol{x}$. The validity of the linearity assumption is of course problem dependent, and that is precisely the focus of the current discussion.

Consider now a nonlinear dynamic system modeled exactly by two alternative systems of nth order differential equations of the form

$$\dot{\boldsymbol{x}} = \boldsymbol{f}(t, \boldsymbol{x}) \qquad \boldsymbol{x}(t_0) = \boldsymbol{x}_0 \qquad \dot{\boldsymbol{y}} = \boldsymbol{g}(t, \boldsymbol{y}) \qquad \boldsymbol{y}(t_0) = \boldsymbol{y}_0 \tag{6}$$

where $\boldsymbol{x}(t)$ and $\boldsymbol{y}(t)$ denote state vectors at time t related by the forward/inverse contact coordinate transformations

$$\boldsymbol{y} = \boldsymbol{G}(\boldsymbol{x}) \qquad \boldsymbol{x} = \boldsymbol{F}(\boldsymbol{y}) \tag{7}$$

Consider also the small departure motion $\delta \boldsymbol{x}(t) = \boldsymbol{x}(t) - \bar{\boldsymbol{x}}(t)$ and $\delta \boldsymbol{y}(t) = \boldsymbol{y}(t) - \bar{\boldsymbol{y}}(t)$ near reference trajectories $\bar{\boldsymbol{x}}(t)$ and $\bar{\boldsymbol{y}}(t)$. The $\delta(\,)$ motions are approximately governed by the linear equations

$$\delta \dot{\boldsymbol{x}} = \left[\frac{\partial \boldsymbol{f}}{\partial \boldsymbol{x}}\right]_{\bar{x}} \delta \boldsymbol{x} \qquad \delta \dot{\boldsymbol{y}} = \left[\frac{\partial \boldsymbol{g}}{\partial \boldsymbol{y}}\right]_{\bar{y}} \delta \boldsymbol{y} \tag{8}$$

$$\delta \boldsymbol{x}(t) = \Phi_x(t, t_0) \delta \boldsymbol{x}(t_0) \qquad \delta \boldsymbol{y}(t) = \Phi_y(t, t_0) \delta \boldsymbol{y}(t_0) \tag{9}$$

where the state transition matrices $\Phi_x = \Phi_x(t, t_0)$ and $\Phi_y = \Phi_y(t, t_0)$ satisfy

$$\dot{\Phi}_x = \left[\frac{\partial \boldsymbol{f}}{\partial \boldsymbol{x}}\right]_{\bar{x}} \Phi_x \qquad \dot{\Phi}_y = \left[\frac{\partial \boldsymbol{g}}{\partial \boldsymbol{y}}\right]_{\bar{y}} \Phi_y \tag{10}$$

with identity matrices as initial conditions.

Now consider the case of uncertain initial conditions on Eqs. (6). Suppose that initial position errors are represented as additive Gaussian errors $\delta \boldsymbol{x}_0$ with known covariance matrix $P_{x_0 x_0}$. Suppose the errors are sufficiently small that the corresponding error covariance matrix of $\delta \boldsymbol{y}_0$ can be determined from linearizing Eq. (7) so we can approximate $P_{y_0 y_0}$ as the static covariance propagation

$$P_{y_0 y_0} = A P_{x_0 x_0} A^T \qquad A \equiv \left.\frac{\partial \boldsymbol{G}}{\partial \boldsymbol{x}}\right|_{x_0} \tag{11}$$

The dynamic propagation of the covariance matrices along the nonlinear trajectories can be computed for the expectations $P_{xx}(t) = E\{\delta \boldsymbol{x}(t) \delta \boldsymbol{x}(t)^T\}$ and $P_{yy}(t) = E\{\delta \boldsymbol{y}(t) \delta \boldsymbol{y}(t)^T\}$ by using linear error theory via the similarity transformations

$$P_{xx}(t) = [\Phi_x(t, t_0)] P_{x_0 x_0} [\Phi_x(t, t_0)]^T \qquad x \to y \tag{12}$$

The 3σ confidence ellipsoids estimated by linear error theory can be computed from the above covariance estimates by substituting directly into Eq. (5). Alternatively, we can transform either of the ellipsoids, at any instant, through the nonlinear coordinate transformations of Eq. (7) and obtain a nonellipsoidal surface. If linear error theory is more valid in the $\boldsymbol{y}$ coordinates than in the $\boldsymbol{x}$ coordinates, then we expect the nonlinearly transformed confidence surfaces to be more valid than the corresponding quadratic surface obtained from linear error theory applied directly to the differential equations for $\delta \boldsymbol{x}$, i.e., the ellipsoid of Eq. (5), using P_{xx} from Eq. (12).

In the context of nonlinear statistics, how do we measure the severity of nonlinearity? We do this by mapping through the nonlinear transformation a set of nonrandom points on the 3σ confidence surface and record the largest departure in a measure of nonlinearity. For example, for a six-dimensional space, we could select the $2n = 12$ points $\boldsymbol{x}_i = \bar{\boldsymbol{x}} + \delta \boldsymbol{x}_i$ at the $\pm$ ends of the semiaxes of the 3σ hyperellipsoid. More generally, the idea is to select a finite number of extreme points that collectively constitute a set of worst cases. Linearity means the Jacobian would be everywhere constant, and this extreme sample should provide a conservative basis for evaluating the variations of the Jacobian as a measure of nonlinearity. We introduce measures of static and dynamic nonlinearity. The static index is for nonlinear coordinate transformations, whereas the dynamic index is for nonlinear differential equations. For the static transformation of Eq. (7), we define the following static nonlinearity index:

$$\nu_s \equiv \sup_i \frac{\|A(\bar{\boldsymbol{x}} + \delta \boldsymbol{x}_i) - A(\bar{\boldsymbol{x}})\|_2}{\|A(\bar{\boldsymbol{x}})\|_2} \tag{13}$$

Solving the nonlinear differential equations (6), from the finite set, e.g., $2n$, of initial conditions $\boldsymbol{x}_i(t_0) = \bar{\boldsymbol{x}}(t_0) + \delta \boldsymbol{x}_i(t_0)$ on the 3σ initial error ellipsoid, we denote the state transition matrix evaluated at time t along the ith trajectory $\boldsymbol{x}_i(t)$ as $\Phi_i(t, t_0) = \partial \boldsymbol{x}_i(t)/\partial \boldsymbol{x}(t_0)$, where $\Phi(t, t_0) = \partial \boldsymbol{x}(t)/\partial \boldsymbol{x}(t_0)$ is evaluated along the nominal or expected trajectory $\bar{\boldsymbol{x}}(t)$. We define the dynamic nonlinearity index $\nu(t, t_0)$ to measure the relative variation of $\Phi_i(t, t_0)$ as follows:

$$\nu(t, t_0) \equiv \sup_i \frac{\|\Phi_i(t, t_0) - \Phi(t, t_0)\|_2}{\|\Phi(t, t_0)\|_2} \tag{14}$$

Here, we abbreviate $\Phi_x(t, t_0)$ and $\Phi_y(t, t_0)$ as $\Phi(t, t_0)$, with the understanding that there is an equation of the form of Eq. (14) for each coordinate choice.

In this context, the sup $(\cdot)$ operator extracts the maximum value of $(\cdot)$ over the finite set of $2n$ points sampled at time t [on the trajectories $\boldsymbol{x}_i(t)$, which ensue from the initial conditions from the $2n$ extrema selected from the surface of the initial 3σ hyperellipsoid], and $\|\cdot\|_2$ denotes the Frobenious norm of a matrix.

C. Nonlinearity Indices: Numerical Results

Using the static indices, we first verify that the small initial covariance matrices can be reliably mapped between coordinate sets by using the similarity transformation in the form of Eq. (11) because the largest value of ν_s for transforming between rectangular coordinates, polar coordinates, and orbit elements is initially found to be $\sim 10^{-3}$. We note that subsequent growth of the error volume results in much larger static indices, however. More importantly, the time history of the three dynamic indices defined in Eq. (14) corresponding to linearizing the dynamics about the nominal orbit for the three coordinate choices show large variations (Fig. 7). It is evident that $\nu(t, t_0)$ varies by an order of magnitude, and this can be used to anticipate that covariance approximations made by using the linearized rectangular coordinate differential equations are less valid

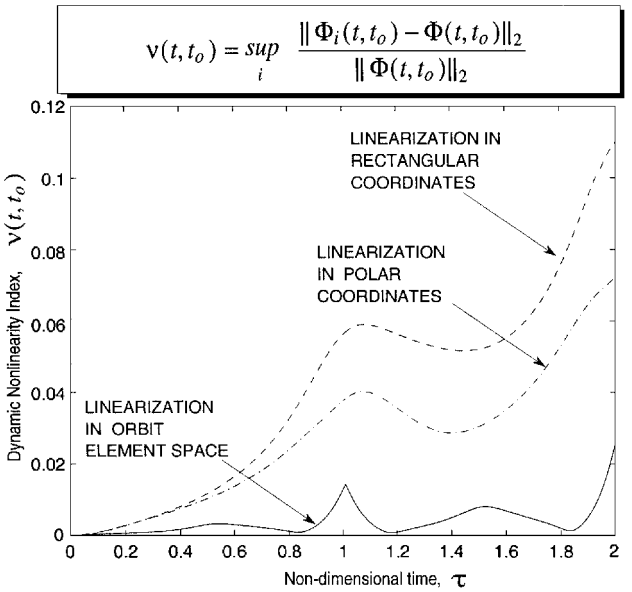

Fig. 7 Dynamic nonlinearity indices: two-orbit variation of $\nu(t, t_0)$ for three coordinate choices.

than those based on the linearized polar coordinate differential equations, which in turn are less valid than covariance approximations made by using the linearized orbit element differential equations. In fact, over two full orbits, a maximum of ~2% variation in $\Phi(t, t_0)$ and an average of only ~0.4% suggests that linear error theory in orbit element space approximates well the actual error dynamics. Observe the qualitatively appealing characteristic of all three ν trajectories in Fig. 7. The motion is significantly more nonlinear near perigee passage where gravitational and drag nonlinearities are a maximum on the nominal orbit. When the confidence ellipsoids from the orbit element space are nonlinearly mapped into rectangular coordinates, we see that they indeed are in excellent agreement with the 200 Monte Carlo trajectories (Fig. 5). See Ref. 48 for the three dynamic equations in the form of Eqs. (6), coordinate transformations in the form of Eqs. (7), and complete discussion of this application. In the next subsection, we demonstrate that the same methodology also applies well to attitude dynamics, and, from these applications, we can see the generality of this approach.

D. Error Propagation in Rotational Kinematics

Substantial historical effort has led to a wide family of coordinate sets for representing angular motion.[3,50] For a given time history of angular velocity $\omega(t) = [\omega_1(t), \omega_2(t), \omega_3(t)]^T$, the orientation history is described exactly by many alternative sets of kinematic differential equations. Frequently, the Euler parameters (quaternions), the Euler angles, the Rodrigues parameters, and the modified Rodrigues parameters are used to parameterize the attitude kinematics.

1. *Euler Parameters*

To make the discussion specific, consider the direction cosine matrix that projects orthogonal body unit vectors $\{\hat{\boldsymbol{b}}\}$ onto space-fixed orthogonal unit vectors $\{\hat{\boldsymbol{n}}\}$ in the sense $\{\hat{\boldsymbol{b}}\} = [C]\{\hat{\boldsymbol{n}}\}$. Let Φ denote the principal rotation angle and $\hat{\boldsymbol{e}}$ be a unit vector along the axis of principal rotation (Euler's theorem).[3]

The Euler parameters are defined as

$$\beta_0 = \cos(\Phi/2) \qquad \beta_i = \hat{e}_i \sin(\Phi/2) \qquad i = 1, 2, 3 \quad (15)$$

This redundant four-dimensional parameterization satisfies the constraint $\beta_0^2 + \beta_1^2 + \beta_2^2 + \beta_3^2 = 1$ and also satisfies the following elegant bilinear differential equation:

$$\begin{Bmatrix} \dot{\beta}_0 \\ \dot{\beta}_1 \\ \dot{\beta}_2 \\ \dot{\beta}_3 \end{Bmatrix} = -\frac{1}{2} \begin{bmatrix} \beta_0 & -\beta_1 & -\beta_2 & -\beta_3 \\ \beta_1 & \beta_0 & -\beta_3 & \beta_2 \\ \beta_2 & \beta_3 & \beta_0 & -\beta_1 \\ \beta_3 & -\beta_2 & \beta_1 & \beta_0 \end{bmatrix} \begin{Bmatrix} 0 \\ \omega_1 \\ \omega_2 \\ \omega_3 \end{Bmatrix} \quad (16)$$

The constraint $\beta_0^2 + \beta_1^2 + \beta_2^2 + \beta_3^2 = 1$ is an exact integral of this equation.

2. *Euler 3-2-1 Angles*

The transformation from the Euler angles $\Theta(t) = [\phi(t), \theta(t), \psi(t)]^T$ to the Euler parameters, with the abbreviations ($s \equiv \sin$, $c \equiv \cos$, $t \equiv \tan$), is defined by

$$\beta_0 = c\frac{\phi}{2}c\frac{\theta}{2}c\frac{\psi}{2} + s\frac{\phi}{2}s\frac{\theta}{2}s\frac{\psi}{2} \qquad \beta_1 = c\frac{\phi}{2}c\frac{\theta}{2}s\frac{\psi}{2} - s\frac{\phi}{2}s\frac{\theta}{2}c\frac{\psi}{2}$$

$$\beta_2 = c\frac{\phi}{2}s\frac{\theta}{2}c\frac{\psi}{2} + s\frac{\phi}{2}c\frac{\theta}{2}s\frac{\psi}{2} \qquad \beta_3 = s\frac{\phi}{2}c\frac{\theta}{2}c\frac{\psi}{2} - c\frac{\phi}{2}s\frac{\theta}{2}s\frac{\psi}{2} \quad (17)$$

and the kinematic differential equations associated with the Euler angles take the form

$$\dot{\Theta} = \begin{Bmatrix} \dot{\phi} \\ \dot{\theta} \\ \dot{\psi} \end{Bmatrix} = \frac{1}{c\theta} \begin{bmatrix} 0 & s\psi & c\psi \\ 0 & c\theta c\psi & -c\theta s\psi \\ c\theta & s\theta s\psi & s\theta c\psi \end{bmatrix} \begin{Bmatrix} \omega_1 \\ \omega_2 \\ \omega_3 \end{Bmatrix} \quad (18)$$

The initial conditions on Eq. (18) are denoted $[\phi(t_0), \theta(t_0), \psi(t_0)] = (\phi_0, \theta_0, \psi_0)$. It can be recognized that this parameterization becomes singular at $\theta(t) = \pm\pi/2$, in contrast to the globally nonsingular Euler parameter kinematic differential equation (16). For the present discussion, the prescribed angular velocities $\omega(t)$ are chosen so that this singular condition is never reached. Thus, Eq. (18) is assumed to remain nonsingular at all times along the trajectories of this example.

Departure motion $\delta\Theta(t) = \Theta(t) - \bar{\Theta}(t)$ in the Euler angles from a nominal trajectory $\bar{\Theta}(t)$ satisfies linearized differential equations derivable by linearizing Eq. (18) [with $\delta\Theta(t_0) \equiv \Theta_0 - \bar{\Theta}_0$]:

$$\delta\dot{\Theta} = \frac{1}{c\theta} \begin{bmatrix} 0 & (s\psi\omega_2 + c\psi\omega_3)t\theta & (c\psi\omega_2 - s\psi\omega_3) \\ 0 & 0 & -(s\psi\omega_2 + c\psi\omega_3) \\ 0 & \dfrac{(s\psi\omega_2 + c\psi\omega_3)}{c\theta} & (c\psi\omega_2 - s\psi\omega_3)s\theta \end{bmatrix}_{\bar{\Theta}} \delta\Theta \quad (19)$$

3. *Rodrigues Parameters*

The Rodrigues parameters eliminate the constraint associated with the Euler parameters by introducing the ratio of the Euler parameters as new coordinates:

$$q_i \equiv \beta_i/\beta_0 \qquad i = 1, 2, 3 \quad (20)$$

Letting $\boldsymbol{q}(t) = [q_1(t), q_2(t), q_3(t)]^T \in \mathcal{R}^3$, the kinematic equations associated with the Rodrigues parameters are derivable from Eq. (16) and take the form

$$\dot{\boldsymbol{q}} = \tfrac{1}{2}[I + [\tilde{\boldsymbol{q}}] + \boldsymbol{q}\boldsymbol{q}^T]\omega \qquad \boldsymbol{q}(t_0) = \boldsymbol{q}_0 \quad (21)$$

where I denotes the 3×3 identity matrix and the symbol $[\tilde{\cdot}]$ denotes the 3×3 skew-symmetric matrix

$$[\tilde{\boldsymbol{q}}] = \begin{bmatrix} 0 & q_3 & -q_2 \\ -q_3 & 0 & q_1 \\ q_2 & -q_1 & 0 \end{bmatrix} \quad (22)$$

The vector $\boldsymbol{q}$ of the Rodrigues parameters is related to the principal eigenaxis $\hat{\boldsymbol{e}}$ and rotation angle Φ as

$$\boldsymbol{q} = \hat{\boldsymbol{e}} \tan(\Phi/2) \quad (23)$$

As is evident from Eq. (23), the Rodrigues parameters cannot be used to describe principal rotations of more than π. To provide a simple nonlinear motion that does not encounter singularities for any of the parameterizations, we consider a prescribed angular velocity vector $\omega(t)$ so that $|\Phi| < \pi$ is satisfied at all times. From Eq. (21), the linearized departure motion $\delta\boldsymbol{q}(t) = \boldsymbol{q}(t) - \bar{\boldsymbol{q}}(t)$ from a nominal set of Rodrigues parameters $\bar{\boldsymbol{q}}(t)$ is governed by

$$\delta\dot{\boldsymbol{q}} = \tfrac{1}{2}\{\omega\boldsymbol{q}^T + (\omega^T\boldsymbol{q})I - [\tilde{\omega}]\}_{\bar{\boldsymbol{q}}}\delta\boldsymbol{q} \quad (24)$$

4. Modified Rodrigues Parameters

If, instead of using Eq. (20), one eliminates the Euler parameter constraint by the transformation

$$\sigma_i = \beta_i/(1+\beta_0) \equiv \hat{e}_i \tan(\Phi/4) \qquad i = 1, 2, 3 \tag{25}$$

the result is the following set of differential equations for the modified Rodrigues parameter vector $\sigma(t) = [\sigma_1(t), \sigma_2(t), \sigma_3(t)]^T \in \mathcal{R}^3$:

$$\dot{\sigma} = \tfrac{1}{4}\{(1-\sigma^T\sigma)I + 2[\tilde{\sigma}] + 2\sigma\sigma^T\}\omega \qquad \sigma(t_0) = \sigma_0 \tag{26}$$

Both the classic [Eq. (20)] and the modified [Eq. (25)] Rodrigues parameters can be derived from the Euler parameters via stereographic projection.[51] The modified Rodrigues parameters, although very closely related to the Rodrigues parameters, are much superior to them with regard to singularity avoidance, because they are not limited to rotations of $|\Phi| < \pi$. A direct transformation from the modified Rodrigues parameters to the Rodrigues parameters can be expressed as

$$\boldsymbol{q} = \left(\frac{\tan\Phi/2}{\tan\Phi/4}\right)\sigma \equiv \left(\frac{2}{1-\sigma^T\sigma}\right)\sigma \tag{27}$$

For $|\Phi| < \pi/2$, we have $\sigma \approx \frac{1}{2}\boldsymbol{q} \approx \frac{1}{4}\Phi\hat{\boldsymbol{e}}$, with the approximation becoming exact as $|\Phi| \to 0$ and becoming poor for $|\Phi| \gg \pi/2$. Moreover, for a given principal rotation angle Φ, $\tan(\Phi/4) \approx \Phi/4$ is clearly a much better approximation than $\tan(\Phi/2) \approx \Phi/2$, so we anticipate σ kinematics to linearize with smaller errors than $\boldsymbol{q}$ kinematics. Thus, in applications where linearization errors are important, we might anticipate it to be advantageous to use the modified Rodrigues parameters rather than the classic Rodrigues parameters. The modified Rodrigues parameters have been generalized further in a recent paper by Tsiotras et al.[52]

Linearized equations (for large ω, small $\delta\sigma \equiv \sigma - \bar{\sigma}$) governing departures in the modified Rodrigues parameters from a nominal motion $\bar{\sigma}(t)$ can be derived from Eq. (26) as

$$\delta\dot{\sigma} = \tfrac{1}{2}\{(\omega^T\sigma)I - [\tilde{\omega}]\}_{\bar{\sigma}}\,\delta\sigma \tag{28}$$

5. Numerical Study of Attitude Error Propagation

For the purpose of illustration, we consider a prescribed angular velocity time history. We choose the nominal Euler angle motion

$$\bar{\phi}(t) = \sin 3t \cos 5t \qquad \bar{\theta}(t) = 0.4\pi \sin 5t$$
$$\bar{\psi}(t) = 0.5 \cos 5t\,\{0.1 + \sin 3t\}^3 \tag{29}$$

It can be readily recognized, for this motion, that $\bar{\Theta}(t)$ never takes the values $\pm\pi/2$ and thus the chosen nominal Euler angles do not encounter singularities in Eqs. (18). The nominal angular rates $\dot{\bar{\Theta}}(t)$ can be obtained by straightforward differentiation of Eq. (29) with respect to time, and from Eqs. (18) we can obtain the corresponding angular velocities

$$\begin{Bmatrix}\omega_1\\ \omega_2\\ \omega_3\end{Bmatrix} = \begin{bmatrix}\sin\bar{\theta}\sin\bar{\psi} & \cos\bar{\psi} & 0\\ \cos\bar{\theta} & 0 & 1\\ -\sin\bar{\theta}\cos\bar{\psi} & \sin\bar{\psi} & 0\end{bmatrix}\begin{Bmatrix}\dot{\bar{\phi}}\\ \dot{\bar{\theta}}\\ \dot{\bar{\psi}}\end{Bmatrix} \tag{30}$$

The history of the body components of $\omega(t)$ for time $0 < t < 10$ is shown in Fig. 8.

The Euler principal rotation angle is obtained from the direction cosine matrix from $\cos\Phi = [\mathrm{tr}(C) - 1]/2$. For the choice of the angular velocities we made earlier, $|\Phi| < \pi$ and hence neither the Rodrigues parameters nor the modified Rodrigues parameters encounter a singularity.

In Fig. 9, we present the time histories of the nominal Euler angles defined in Eq. (29) and the corresponding nominal Rodrigues parameters and nominal modified Rodrigues parameters. To expose the effect of various attitude coordinate choices on the validity of linear error propagation, 200 Monte Carlo initial errors were simulated by using a Gaussian random number generator with an initial error standard deviation of 2 deg in the Euler angles. Initial errors

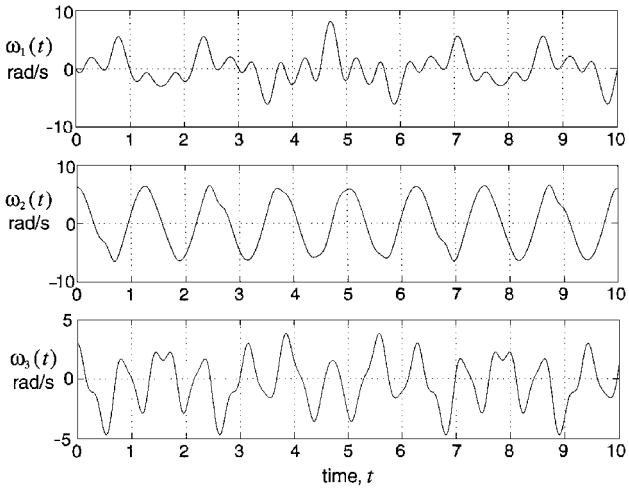

Fig. 8 Angular velocity history in body axes.

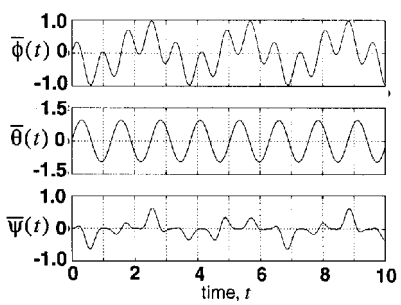

Nominal Euler 3-2-1 angles

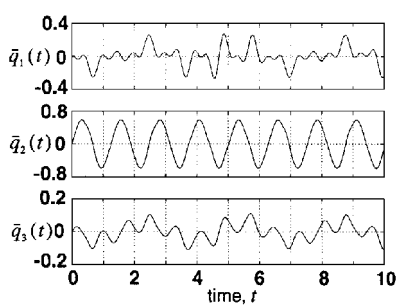

Nominal Rodrigues parameters

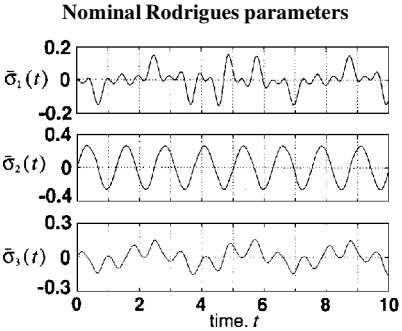

Nominal modified Rodrigues parameters

Fig. 9 Nominal motion: Euler angles $\bar{\Theta}(t)$, Rodrigues parameters $\bar{q}(t)$, and modified Rodrigues parameters $\bar{\sigma}(t)$.

in the three angles are assumed to be statistically independent. Before discussing the dynamic error propagation results, we consider the validity of mapping initial uncertainty prescribed in the Euler angles to the Rodrigues parameters and the modified Rodrigues parameters, so we can establish consistent initial uncertainties in all three coordinate sets. The static nonlinearity index ν_s at time $t = 0$ was computed from Eq. (13) for the various coordinate transformations; the largest value of ν was $\approx 10^{-3}$. It is therefore evident that the static index of nonlinearity is "small" for all the static transformations over the given volumes of uncertainty $\Rightarrow$ we conclude that Gaussian statistics prescribed in the original coordinates (Euler

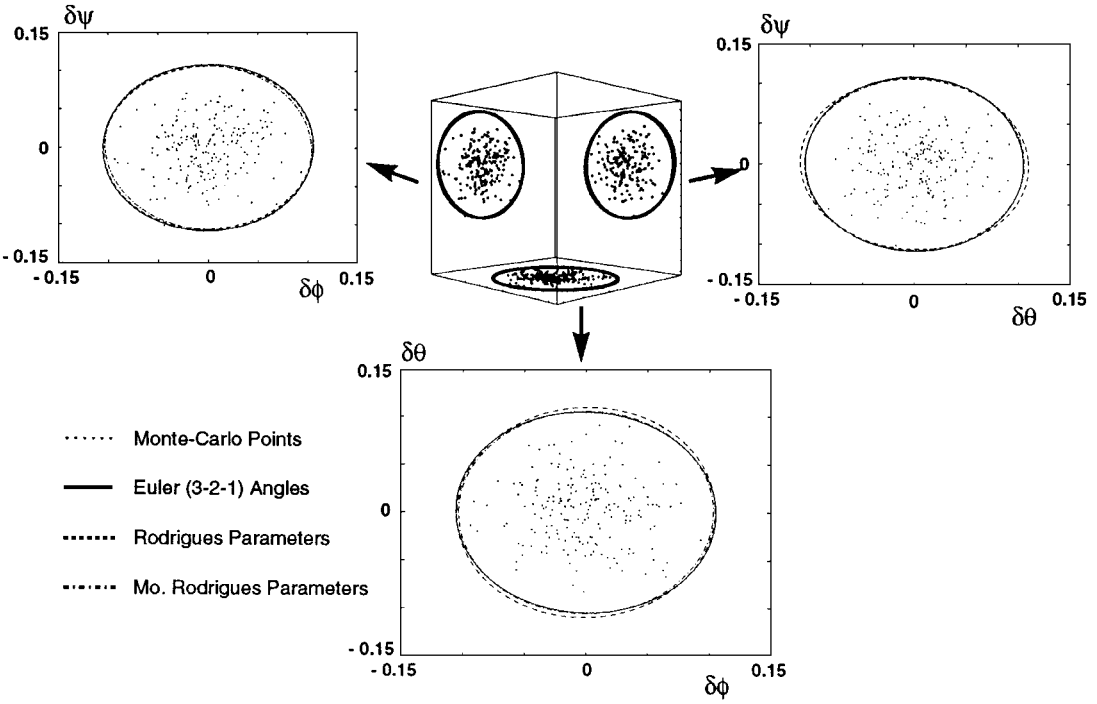

Fig. 10 A 3σ confidence surfaces snapshot at $t = 0.0$ s.

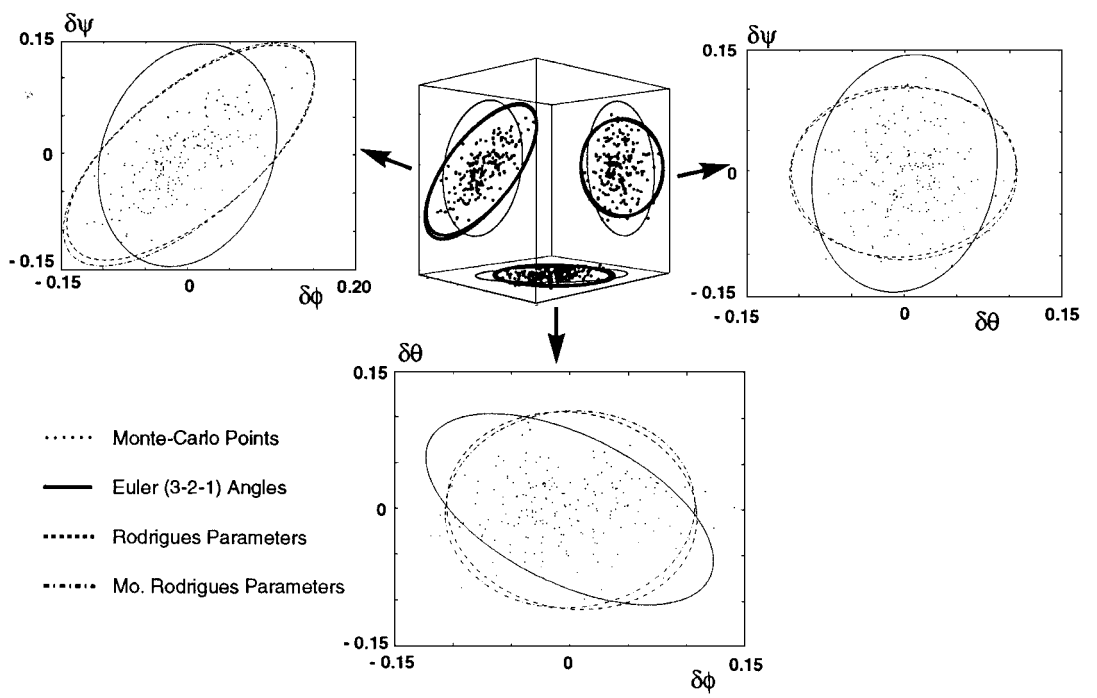

Fig. 11 A 3σ confidence surfaces snapshot at $t = 0.5$ s.

angles) are mapped with good approximation to Gaussian statistics in the Rodrigues parameters and modified Rodrigues parameters.

During simulations, uncertainty is propagated with Eq. (12) for all three coordinate sets. Three snapshots of the 3σ constant probability surfaces at $t = 0, 0.5$, and 9.5 s from linear error theory are shown in Figs. 10–12. The two Rodrigues ellipsoidal 3σ surfaces are mapped into corresponding nonellipsoidal surfaces in the Euler angle space. All three 3σ surfaces of constant probability are displayed, along with the 200 Monte Carlo simulation points; for ease of visualization, projections of the 3σ surfaces and the Monte Carlo integrated points into the $(\delta\phi, \delta\theta)$, $(\delta\phi, \delta\psi)$, $(\delta\theta, \delta\psi)$ planes are shown. For very early evolutions of the nonlinear probability distribution of errors, the linear error theory uncertainty propagation is valid for all three coordinate sets.

Figures 11 and 12 indicate that the longer-term prediction of the 3σ surface from propagation in the Rodrigues parameters and the modified Rodrigues parameters captures the true nature of the actual nonlinear/non-Gaussian error distribution in Euler angle space to a much better degree when compared with direct linear error theory propagation by using the linearized Euler angle differential equations. The performance of linear error theory in different coordinates can be anticipated without the expense of a Monte Carlo process by computing the dynamic nonlinearity index $\nu(t, t_0)$ for the three coordinate systems as a function of time (Fig. 13). The computations of $\nu(t, t_0)$ are based on 12 initial conditions chosen from the initial 3σ error ellipsoid. The linearization-based predictions using Rodrigues parameters and modified Rodrigues parameters compared favorably with Monte Carlo calculations (errors $<1\%$), whereas linearization

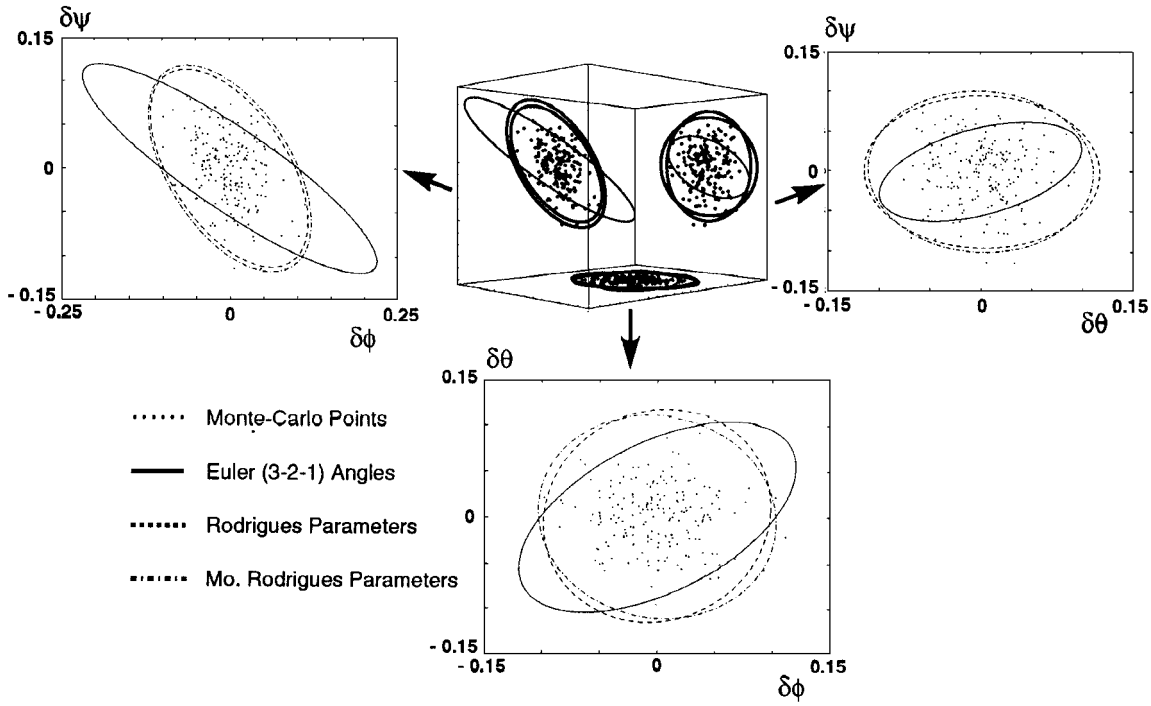

Fig. 12 A 3σ confidence surfaces snapshot at $t = 9.5$ s.

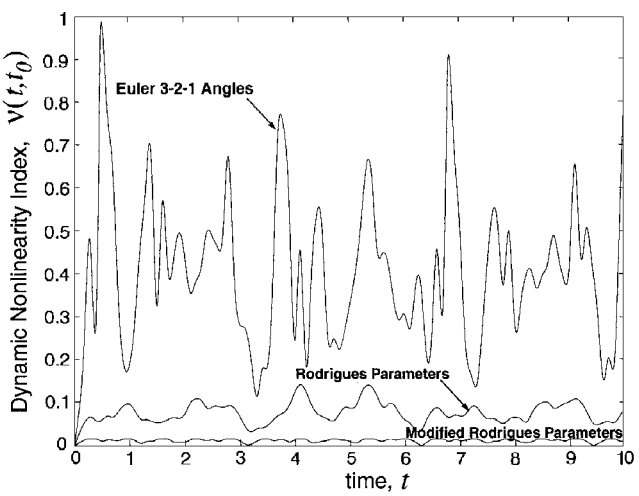

Fig. 13 Dynamic nonlinearity index variation.

approximations in the Euler angles were very erratic with errors ranging from ~20 to ~100%.

Figures 7 and 13 provide clear evidence that not all linearizations are created equal. For both orbital mechanics and attitude dynamics ⇒ evaluating the linearity indices allows confident decisions between competing coordinate choices vis-à-vis applicability of linear error theory. These results have significant implications in applications of estimation and control theory. For example, the linearity and Gaussian assumptions underlying Kalman filter design strongly favor the modified Rodrigues parameters over any set of Euler angles. Also of interest, optimal control theory is routinely applied to regulate nonlinear systems near a target state; it is evident that the quantitative and qualitative ideas introduced for assessing the validity of the underlying linearity assumptions (and therefore the optimality of the resulting controller design) is of broad significance in control of dynamic systems.

III. Quasicoordinates for Multibody Systems

We now turn to another coordinate-related issue in dynamic systems. Consider the class of nonlinear dynamic systems whose kinetic energy (T) has the structure

$$T = \tfrac{1}{2}\dot{\boldsymbol{x}}^T[M(\boldsymbol{x})]\dot{\boldsymbol{x}} + T_1(t, \boldsymbol{x}, \dot{\boldsymbol{x}}) + T_0(t, \boldsymbol{x}) \tag{31}$$

where $\boldsymbol{x}(t) \in \mathcal{R}^n$ is a configuration vector of independent generalized coordinates, $M(\boldsymbol{x}) = M^T(\boldsymbol{x}) \in \mathcal{R}^{n\times n}$ is a positive definite configuration-variable mass matrix, $T_1(t, \boldsymbol{x}, \dot{\boldsymbol{x}})$ depends linearly on $\dot{\boldsymbol{x}}$, and $T_0(t, \boldsymbol{x})$ does not contain $\dot{\boldsymbol{x}}$. For this class of systems, being acted on by control forces $\boldsymbol{u}(t) \in \mathcal{R}^m$, the differential equations can be brought to the form

$$M(\boldsymbol{x})\ddot{\boldsymbol{x}} = F(t, \boldsymbol{x}, \dot{\boldsymbol{x}}, \boldsymbol{u}) \tag{32}$$

We assume that the mass matrix $M = M^T > 0$ is an analytic function of $\boldsymbol{x}(t)$, and $F(t, \boldsymbol{x}, \dot{\boldsymbol{x}}, \boldsymbol{u}) \in \mathcal{R}^n$ is a continuous function of all arguments. It is evident that any discontinuity in the arbitrary control inputs $\boldsymbol{u}(t)$ can instantaneously affect $\ddot{\boldsymbol{x}}(t)$ but not $\dot{\boldsymbol{x}}(t)$ or $\boldsymbol{x}(t)$. Therefore, $M = M(\boldsymbol{x}, \dot{\boldsymbol{x}})$ is also continuous, but $\dot{M} = \dot{M}(\boldsymbol{x}, \dot{\boldsymbol{x}}, \ddot{\boldsymbol{x}})$ may be discontinuous, depending on $\boldsymbol{u}(t)$. For any instant t, we observe that M can be decomposed into its spectral factors C, and Λ as

$$M = C^T\Lambda C \Leftrightarrow \Lambda = CMC^T \tag{33}$$

where $\Lambda = \text{diag}(\lambda_i)$ and $C^T \in \mathcal{R}^{n\times n}$ is the orthogonal matrix of eigenvectors. Obviously, because $M = M[\boldsymbol{x}(t)]$, Λ and C are implicitly time-varying functions of $\boldsymbol{x}(t)$. Except for possibly near repeated λ_i values, we anticipate that both Λ and C will be smooth functions of $\boldsymbol{x}(t)$. It is evident that if we can generate $C(t)$ and $\Lambda(t)$ by solving differential equations governing their time evolution, then because of the orthogonality of $C(C^TC = CC^T = I)$, we can avoid the necessity of numerically inverting the large configuration-variable $M[\boldsymbol{x}(t)]$, because $M^{-1} = C^T\Lambda^{-1}C$. Since $M = M^T > 0$, the eigenvalues λ_i will always be positive. Because $\lambda_i > 0$, we can always define $s_i = \sqrt{\lambda_i}$ and the corresponding matrix $S = \text{diag}(s_i)$. This allows M to be factored as $M = C^TS^TSC = W^TW$, where $W = SC$ is the matrix square root of M. Therefore, keeping track of C and S is equivalent to a square root algorithm with most of the advantages.[53] The algorithm presented by Oshman and Bar-Itzhak,[53] however, is not robust if there are repeated crossings of the eigenvalues of $M[\boldsymbol{x}(t)]$, we discuss a way to solve this problem. Note that the inverse of M is alternatively written $M^{-1} = C^TS^{-2}C$.

In a recent study,[54] we found it attractive to introduce a quasi-coordinate velocity transformation

$$\boldsymbol{v}(t) = SC\dot{\boldsymbol{x}}(t) \Rightarrow \dot{\boldsymbol{x}}(t) = C^TS^{-1}\boldsymbol{v}(t) \tag{34}$$

satisfying the dynamic equation

$$\dot{\boldsymbol{v}} = S^{-1}CF(t, \boldsymbol{x}, \dot{\boldsymbol{x}}, \boldsymbol{u}) + (\dot{S} - S\Omega)S^{-1}\boldsymbol{v} \tag{35}$$

To make the preceding differential equation most useful, we require means for continuously computing the eigenfactors S, C. Recent papers[6,53–61] have established the insight needed to write the following differential equations for C and S:

$$\dot{C} = -\Omega C \qquad \text{and} \qquad \dot{S} = \tfrac{1}{2}\Gamma S^{-1} \tag{36}$$

$$\Omega^T = -\Omega \qquad S = \text{diag}(s_i) \qquad \Gamma = \text{diag}(\mu_{ii}) \tag{37}$$

where

$$[\mu_{ij}] = C\dot{M}C^T \tag{38}$$

$$\Omega_{ij} = \frac{\mu_{ij}}{\left(s_j^2 - s_i^2\right)} \qquad \text{for} \qquad s_j \neq s_i \tag{39}$$

For the case of near-repeated eigenvalues, it is necessary to introduce a stabilization method to integrate Eqs. (34–36). This can be accomplished by using differential Jacobi rotations to establish (C, S) correctors for integration steps near repeated eigenvalues.[54]

We note that the bulk of the computational effort is the matrix product ($[\mu_{ij}] = C\dot{M}C^T$), but because in reality each μ_{ij} is an independently computable inner product of rows of C with $\dot{M}\Rightarrow$, this process is inherently parallelizable in contrast to, for example, a solution for $\ddot{x}$ in Eq. (32). This property enables this approach to be easily mapped onto massively parallel machines to be employed on a large class of high-dimensioned nonlinear multibody dynamics and large dynamic deployment/reconfiguration problems.

For the analogous problem of spacecraft attitude kinematics, $C \in \mathcal{R}^{3\times 3}$ is the orthogonal direction cosine matrix and the distinct elements of Ω_{ij} are the body components of angular velocity. So this line of thinking lifts $C(t) \in \mathcal{R}^{3\times 3}$ rotational kinematics to analogous kinematic equations that describe the evolution of higher dimensioned orthogonal matrices $C(t) \in \mathcal{R}^{n\times n}$, which locally factor the symmetric positive definite mass matrix.

We note that near-repeated eigenvalues indicate symmetry conditions in which the principal axes of M and therefore the corresponding rows of C are not generally unique. However, we observe[54] that C, $\dot{C}$, S, $\dot{S}$ must generate M and $\dot{M}$. $\Rightarrow$ The $\dot{M}$ requirement usually makes the eigenvectors (C) unique (unless $\lambda_j \to \lambda_i$ and $\dot{\lambda}_j \to \dot{\lambda}_i$ occur simultaneously, i.e., not merely eigenvalue crossing but the more rare event of eigenvalue osculation). Numerical difficulties will occur in some $\lambda_j \to \lambda_i$ situations, however, and a stabilization scheme is needed to solve Eqs. (36) robustly. Invoking quadratically convergent differential Jacobi rotations[54] near repeated eigenvalues modifies the approximation for C and S, as needed, to track both $M(t)$ and $\dot{M}(t)$ smoothly. As a practical matter, the occasional local loss of uniqueness of C is not as troublesome as it might first appear, because the algorithm validity relies on the convergence to any instantaneously diagonalizing transformation.

To provide some insight to the potential significance of the above developments, we consider an example.[62] Shown in Fig. 14 is a simple multibody problem; the mass matrix of this two-degree-of-freedom system depends on the cosine of the elbow angle. We show in Fig. 15 the free nonlinear response of this system.

We consider the nonlinear free vibration problem starting from the initial conditions: $\theta_1(0) = 0$, $\theta_2(0) = 60$ deg, $\dot{\theta}_i(0) = 0$. For simplicity, the unstretched spring length is taken as zero. The initial configuration is not an equilibrium position; this conservative system will therefore undergo nonlinear free vibration with a known exact energy integral. Errors in this exact energy integral can be used as a rigorous measure of integration stability. The system parameters, constraint conditions, and initial conditions were varied to study effects of nonlinear snap-through motions and near-repeated mass matrix eigenvalues. For the case of constrained motion (Fig. 14), the mass matrix eigenvalues crossed once on each oscillation.

The focus of this example is on stability of the algorithm, and even this simple case shows clear advantages. The numerical solution was computed by a standard fourth-order Runge–Kutta algorithm, and, for especially simple discussion, we did not make use of the usual variable step size control one would employ for problems with a nonlinear acceleration history. Referring to Fig. 15, note the remarkable enhancement of the numerical solution achieved through

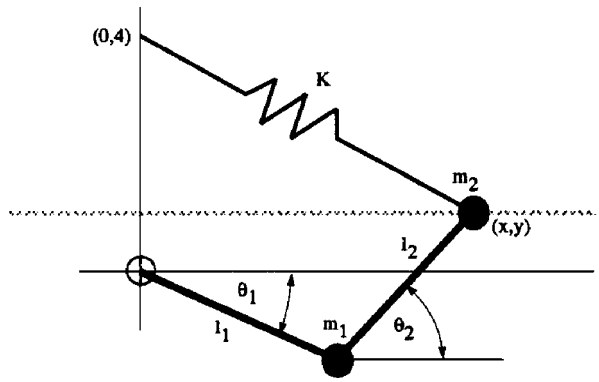

Nonlinear mechanism

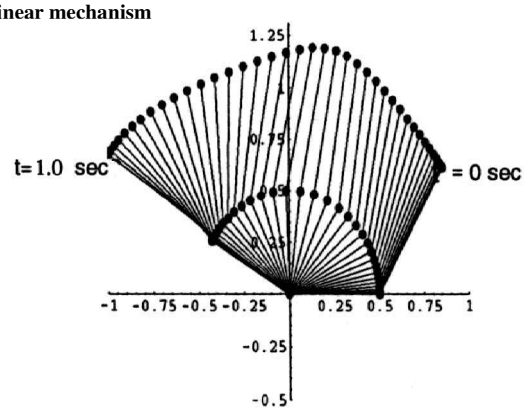

Unconstrained free response

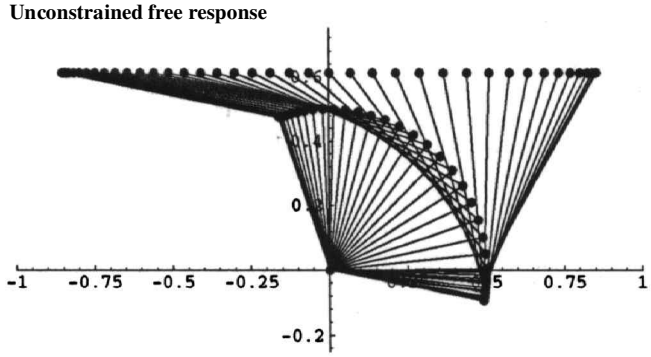

Constrained free response

Fig. 14 Conservative nonlinear multibody system.

the use of the preceding quasicoordinate formulation (method 1), in comparison to direct integration (method 3) of angular accelerations by inverting Eq. (32). Method 2 is a hybrid in which the $[C(t),\ S(t)]$ solution is used to algebraically generate the inverse of $M(\boldsymbol{x})$, but angular acceleration is integrated instead of the quasicoordinate vector. The quasicoordinate accelerations are much smoother than the angular accelerations, especially near elbow snap-throughs, and the resulting integration is three orders of magnitude more precise than method 3 and almost one order of magnitude more precise than method 2 for any given step size. Note further that the ultimate precision is improved dramatically over the traditional method 3, again by three orders of magnitude in this low degree of freedom example, and this approach has shown exceptional stability on all examples studied to date.

IV. Feedback Control of Attitude Maneuvers

During the past two decades, there has been an exciting series of dynamics/controls adventures that address various aspects of how to maneuver a spacecraft from orientation state A to orientation state B. Before the 1980s, most attitude control laws were designed based on linearized dynamics and uncoupled one-loop-at-a-time yaw-pitch-roll control design strategies. Because spacecraft were mostly rigid and maneuvers were usually slow, these idealizations were sufficient to solve practical problems and led to sufficiently robust control laws that could be implemented in available computers. The advent of

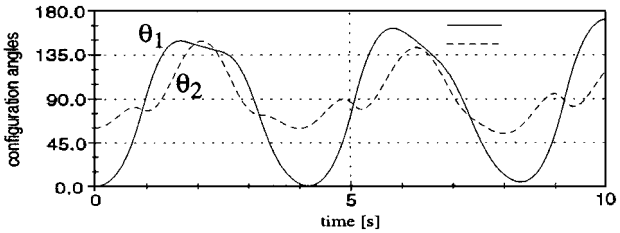

a) Angular response history is characterized by frequent elbow snap-throughs where the $\theta_1 = \theta_2$; these snap-through events are characterized by high-jerk (large $d^3\theta/dt^3$) regions

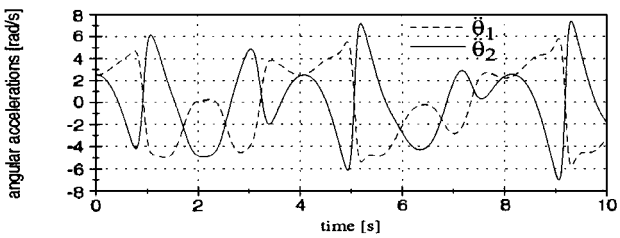

b) Angular acceleration is very nonlinear because of the high-jerk regions near every elbow snap-through; one would anticipate smaller step sizes in these regions to maintain integration accuracy

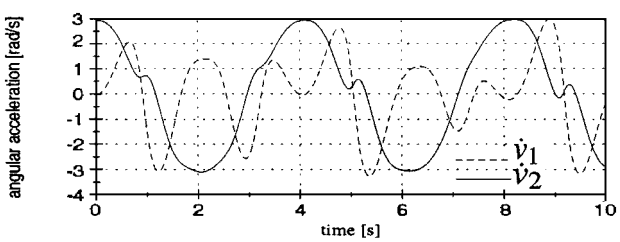

c) Quasicoordinate acceleration history is smoother than the $\ddot{\theta}(t)$ history, especially $\Rightarrow$ near elbow snap-throughs, anticipate larger step sizes for a given accuracy $\Rightarrow$ $\surd$effect

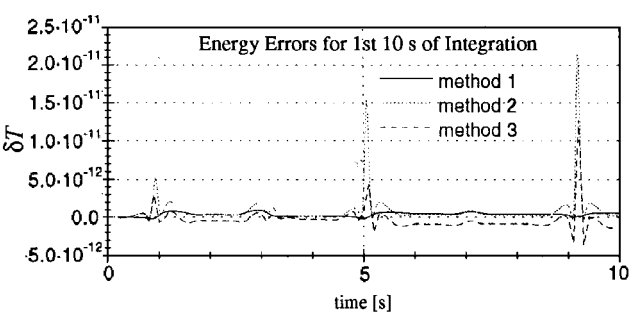

d) Integration was done with a fixed step size; note the maximum errors $\sim$ snap-throughs; three methods, solve: method 1, $\dot{v} = S^{-1}CF(\theta) + (\dot{S} - S\Omega 1)\, S^{-1}v$; method 2, $\ddot{\theta} = C^T S^{-2} CF(\theta)$; and method 3, $\ddot{\theta} = M^{-1}F(\theta)$

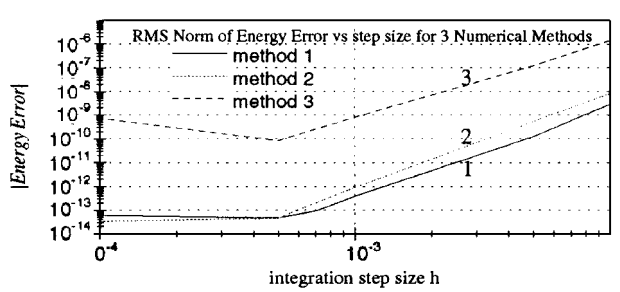

e) Long-term stability of integration vs step size is evident; note especially square-root methods, $\Rightarrow$ method 1 is always superior to method 3 (conventional algorithm); ultimate precision is vastly superior

Fig. 15 Nonlinear response.

large flexible structures and requirements for rapid maneuvers and vibration arrest have posed new challenges that have been partially met with an impressive set of recent theoretical, computational, and hardware developments. This family of problems is complicated by several considerations: 1) nonlinearity, 2) structural flexibility, 3) evolutionary variable geometry structures, 4) model uncertainty, 5) high dimensionality, 6) practical limitations on real-time computing, sensor/actuator limitations, and 7) difficulty in defining optimality. Because of the need for autonomy and reliability in the face of these difficulties, these problems have served as a very important technology driver in dynamics and control. As will be evident, mechanics-derived insights have been crucial in determining the most appropriate ways to harness control theory and effect impressive/realizable solutions.

To capture the spirit of some recent analytical developments, consider the attitude dynamics of a rigid spacecraft described by the principal axis form of Euler's rotational equations of motion

$$I_1\dot{\omega}_1 = (I_2 - I_3)\omega_2\omega_3 + u_1 \qquad I_2\dot{\omega}_2 = (I_3 - I_1)\omega_3\omega_1 + u_2$$
$$I_3\dot{\omega}_3 = (I_1 - I_2)\omega_1\omega_2 + u_3 \tag{40}$$

along with the kinematic equations for a chosen set of coordinates. We could choose the Euler angles; however, this would lead to differential equations containing a singularity located no more than $\pi/2$ from the current state. A better selection for large motion control design is any one of the several coordinate sets associated with Euler's principal rotation theorem, e.g., the Euler parameters, the Rodrigues parameters, or the modified Rodrigues parameters. We select the latter set, so the sixth-order system is described by Eqs. (40) and Eqs. (26).

The most important step in applying a Lyapunov approach in control design is the selection of the Lyapunov function to measure errors from the target state. This issue is treated in several texts and recent papers.[3,32,33,43] For the purposes of illustration, we adopt the following Lyapunov function:

$$V = \underbrace{\tfrac{1}{2}\omega^T[\mathrm{diag}(I_i)]\omega} + 2k_0\,\underbrace{\ell n[1 + \sigma^T\sigma]}$$
$$= \overbrace{\text{kinetic energy}} + 2k_0\,\overbrace{\ell n[1 + \tan^2(\Phi/4)]} \tag{41}$$

We note that the Lyapunov function V is positive definite and vanishes only at the target state (the origin). The idea is to find the structure of a global asymptotically stabilizing control law $u_i(\omega_1, \omega_2, \omega_3, \sigma_1, \sigma_2, \sigma_3)$ by requiring u_i to cause $\dot{V}$ to be strictly negative along the closed-loop trajectories of the system. In this case, differentiating Eq. (41) leads directly to the modified power equation

$$\dot{V} = \sum_{i=1}^{3} \omega_i\,(u_i + k_0\,\sigma_i) = \omega^T(\boldsymbol{u} + k_o\,\sigma) \tag{42}$$

$\dot{V}$ can be made nonpositive as follows: because $\boldsymbol{u}$ has not been chosen, the parenthetic term $\boldsymbol{u} + k_0\sigma$ can be constrained so that the sign of $\dot{V}$ is guaranteed to be negative. The simplest stabilizing control law is obtained by setting $\boldsymbol{u} + k_0\,\sigma = -G\omega$; this gives

$$\boldsymbol{u} = -k_0\,\sigma - G\omega \tag{43}$$

where the constant gains $k_0 > 0$ and $G = G^T > 0$ can be selected by some optimization process subject to the positivity requirement. Remarkably, this simple linear feedback law stabilizes the general nonlinear dynamics. The derivative of V is

$$\dot{V} = -\omega^T G\omega \tag{44}$$

Because $\dot{V}$ does not contain σ, it is clear that $\dot{V}$ is negative semidefinite only, and we cannot immediately claim asymptotic stability for the closed-loop dynamics. However, a useful theorem[3,45] says that, if the higher derivatives of V are evaluated on the set Z where $\dot{V} = 0$, and the first nonzero V time derivative is odd and negative definite on Z, then we have asymptotic stability in spite of the apparent possibility that $\dot{V}$ may vanish. Physically, this proves

that the motion does not remain at possible apogee states where $\dot{V}$ kisses zero, because these states are not equilibrium points. In this case, the only equilibrium state of the closed-loop system is the origin, and it can be verified that the first nonzero derivative of V on $\{Z : \omega = 0, \sigma \neq 0\}$ is the third derivative and it is negative definite on Z, so we indeed have asymptotic stability for all states within $\pm 2\pi$ of the target state. It is easy to verify that coordinate selection is crucial in the above process of finding globally stabilizing control laws. We found that a simple linear feedback law gives stability in the large; choosing any set of Euler angles would be an illuminating exercise that would not lead to these elegant results. Over and above the proof of stability, there are other implicit advantages. In particular, because the modified Rodrigues are a very near-linear three-parameter description of motion, the domain of validity of the optimal control gains (if we linearize about the target state and apply optimal linear control theory[3]) is much larger than, for example, any choice of Euler angles. The insight to write the measure of attitude error as $\ell n(1 + \sigma^T \sigma)$ in Eq. (41) is due to Tsiotras.[33]

More generally, analogous recent developments have been carried out for distributed parameter and time-varying systems and validated through analytical, numerical, and laboratory experimental research, and these have been augmented with concepts from adaptive control theory to make this approach robust in the presence of model errors and disturbances.[3,29,30,32,33,43–47,54,63] In particular, the results by Schaub et al.[63] provide key insights into the construction of attitude penalty functions for stability and control analysis to eliminate the usual dependence of the definition of attitude error on the choice of attitude coordinates. We introduced a universal attitude error measure $J = [3 - \mathrm{tr}(C)]/4$, where C is the direction cosine matrix projecting the current body axes onto their target orientation.[63] This positive error measure can be expressed in any coordinate set and, for example, as a function of the principal rotation Φ and $\hat{e}$ is simply $J = \sin^2(\Phi/2)$. Thus, a 180-deg rotation from the target orientation about any axis gives the maximum value of $J = 1$. This function is graphed in Fig. 16.

The marriage of Lyapunov stability theory with controller design methods has resulted in a unified approach that applies to nonlinear, distributed parameter, and time-varying control law design. The developments consider not simply regulation in the vicinity of a fixed-target equilibrium state but also tracking of nonlinear reference maneuvers and model reference adaptive control. The reference maneuvers, in practical applications, are typically designed by rotating about the principal rotation axis (eigenaxis) from the initial target state, with the angular acceleration history of the reference

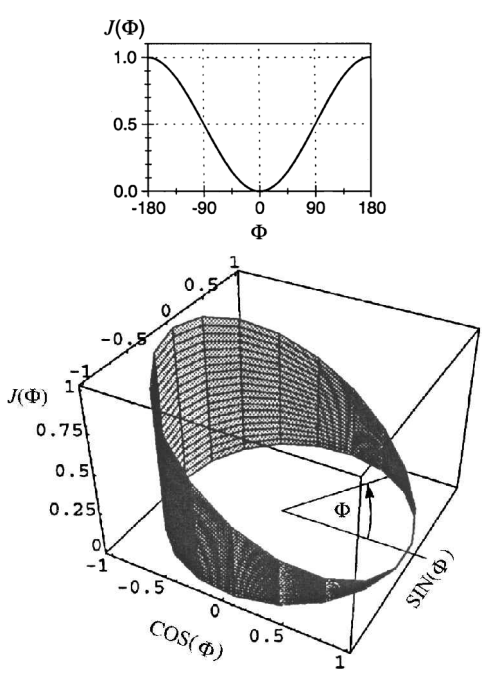

Fig. 16 Universal attitude penalty function.

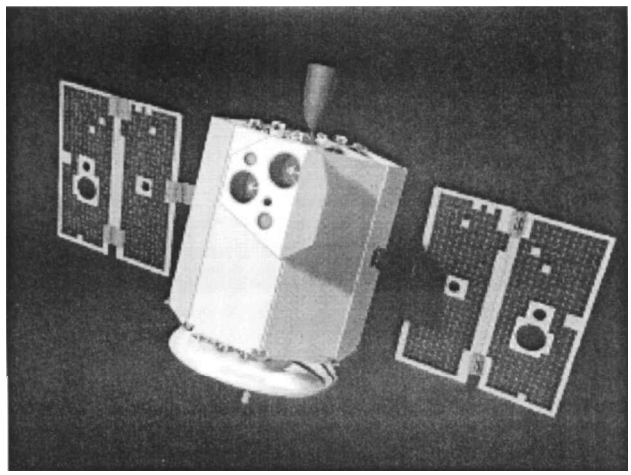

Fig. 17 Clementine spacecraft.

maneuver being specified as bang-bang, bang-off-bang, and torque-shaped variations of these strategies. The tracking feedback laws are designed by using Lyapunov methods to ensure stability and robustness with respect to model errors and disturbances.

To illustrate the maturity of this approach, consider the recent Clementine mission. The Clementine spacecraft, shown in Fig. 17, was launched Jan. 25, 1994. This was the first post-Apollo return to the moon and was primarily a mapping mission with a requirement for numerous large-angle, three-dimensional pointing maneuvers to point the mapping camera to track specific targets of interest on the lunar surface. Attitude control was accomplished by torquing three orthogonal reaction wheels. Attitude estimation made use of two solid-state star cameras and real time, onboard star identification utilizing an approach that represents a refinement of the concepts introduced by Junkins et al.[64,65]; this approach was also utilized in the recently launched near-Earth asteroid rendezvous (NEAR) mission.[65,66]

The attitude control law for Clementine was designed by Creamer and colleagues[31,67] using extensions of methodology developed by Wie and Barba[30] and by Junkins and colleagues.[3,29,43,54] A unique feature of Creamer's approach is the incorporation of integral feedback to null motor friction-induced steady-state errors. The reference maneuvers designed for Clementine were eigenaxis rotations of the near-minimum-fuel bang-off-bang type. Inverse dynamics was used to solve for a reference feedforward torque profile to drive the reaction wheels. Based on real-time state estimation, perturbation feedback control proportional to the error quaternion (Euler parameter) estimates, angular velocity tracking error estimates, and the integral of the error quaternion estimate was superimposed on the feedforward reference torque history. The stability characteristics were analytically verified by Lyapunov analysis and simulation studies. The on-orbit implementation was remarkably successful, with more than 1000 large-angle maneuvers performed without significant anomalies other than occasional maximum wheel-speed saturations. A typical comparison of simulated vs actual on-orbit results is shown in Fig. 18. As is evident, the wheel speeds and quaternions are almost graphically identical to the on-orbit maneuver results. The routineness and precision with which autonomous, large-angle point and track maneuvers could be carried out was central to the success of the Clementine mission. This capability permitted the selective high-resolution optical and radar imaging of many potentially interesting lunar targets. This capability indirectly enabled the discovery of the recently reported[68] ice deposit near the lunar south pole.

The Clementine and NEAR missions clearly demonstrate that by virtue of advances in conceptual understanding, hardware design, and renewal of an aggressive "can-do philosophy," we have entered a new lower cost, higher performance, and shorter development age for small exploratory space missions. The success of these missions indicates that faster, better, and cheaper are not just salesmanship buzz words; they describe the culmination of impressive advances on several fronts. This ongoing evolution promises even greater impact in the future.

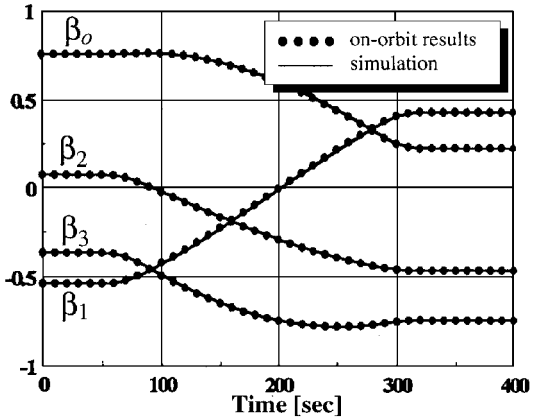

Quaternions

$\Omega_i[rpm]$

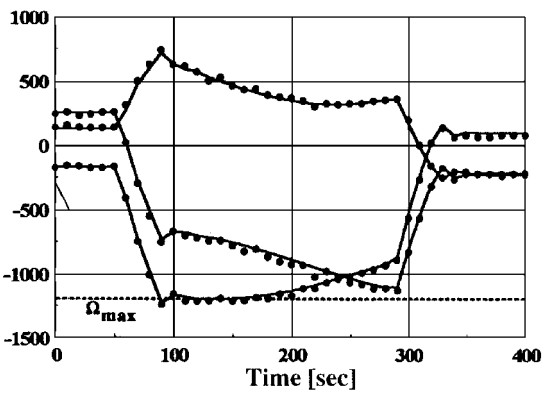

Wheel speeds

Fig. 18 Clementine on-orbit maneuver results.

V. Concluding Remarks

This paper provides an overview of recent progress in spacecraft dynamics, estimation, and control. The discussion synthesizes a broad set of topics and includes analytical and computational research as well as several on-orbit implementations. The presentation emphasizes unified developments in methodology for analytical dynamics, stability, control, and estimation. The primary conclusion that can be drawn from the several adventures discussed is that the field of spacecraft dynamics and control is maturing rapidly $\Rightarrow$ many of the most interesting challenges arise on the traditional disciplinary interfaces.

In preparing this paper, the author has been frequently reminded of the multidimensional joy he has experienced over the past three decades while working in this rapidly changing field, often time-sharing basic research with active involvement in development efforts and missions. Let us never unlearn the lessons of our most dramatic decade of progress (the Apollo era)—theoretical research in dynamics and control methodology and advanced flight implementations not only can comfortably coexist, they belong to the same set.

Acknowledgments

My sponsorship by the following organizations has been vital: the University of Virginia, Virginia Polytechnic Institute, Texas A&M University, NASA, Naval Surface Weapons Center, Sandia National Laboratories, Air Force Office of Scientific Research, Phillips Laboratory, United Space Alliance, Lockheed Martin Corporation, the Johns Hopkins Applied Physics Laboratory, the Texas Advanced Technology Program, and the Texas Engineering Experiment Station. This work has benefited from collaboration with many colleagues. I am delighted to mention the following individuals who have directly contributed to this work: M. R. Akella, K. T. Alfriend, R. H. Bishop, H. D. Black, H. Bang, C. K. Carrington, J. E. Cochran, N. G. Creamer, J. N. Juang, A. J. Kurdila, Y. Kim, V. J. Modi, H. S. Morton, R. Mukherjee, Z. H. Rahman, R. D. Robinett III, H. Schaub, M. D. Shuster, T. E. Strikwerda, P. Tsiotras, J. D. Turner, S. R. Vadali, A. J. Verma, and C. E. Williams. Finally, I have enjoyed working closely with more than 50 graduate students, whose years of inspired scholarship underwrote many of the results discussed here.

References

[1]Hyland, D. C., Junkins, J. L., and Longman, R. W., "Active Control Technology for Large Space Structures," *Journal of Guidance, Control, and Dynamics*, Vol. 16, No. 5, 1993, pp. 801–821.

[2]Meirovitch, L., *Dynamics and Control of Structures*, Wiley-Interscience, New York, 1990.

[3]Junkins, J. L., and Kim, Y., *Introduction to Dynamics and Control of Flexible Structures*, AIAA Education Series, AIAA, Washington, DC, 1993.

[4]Junkins, J. L. (ed.), *Mechanics and Control of Large Flexible Structures*, Vol. 129, Progress in Astronautics and Aeronautics, AIAA, Washington, DC, 1990.

[5]Junkins, J. L., *Dynamics of Large Structures in Space*, Springer–Verlag, Berlin, 1990.

[6]Junkins, J. L., and Turner, J. D., *Optimal Spacecraft Rotational Maneuvers*, Elsevier, Amsterdam, 1986.

[7]Bryson, A. E., *Control of Spacecraft and Aircraft*, Princeton Univ. Press, Princeton, NJ, 1994.

[8]Pars, L. A., *A Treatise on Analytical Dynamics*, Heinemann, London, 1965.

[9]Krener, A. J., "On the Equivalence of Control Systems and the Linearization of Nonlinear Systems," *SIAM Journal on Control and Optimization*, Vol. 11, No. 4, 1973, pp. 670–676.

[10]Hermann, R., and Krener, A. J., "Nonlinear Controllability and Observability," *IEEE Transactions on Automatic Control*, Vol. AC-22, No. 5, 1977, pp. 728–740.

[11]Brockett, R. W., "Feedback Invariants for Nonlinear Systems," *Proceedings of the Sixth IFAC Congress* (Helsinki), AIAA, Washington, DC, 1978, pp. 1115–1120.

[12]Jakubczyk, B., and Respondek, W., "On Linearization of Control Systems," *Bulletin de l'Academie Polonaise des Sciences, Serie des Sciences Mathematiques*, Vol. 28, Nos. 9, 10, 1980, pp. 517–521.

[13]Hunt, R., and Su, L. R., "Linear Equivalents of Nonlinear Time-Varying Systems," *Proceedings of the International Symposium on Math. Theory of Networks and Systems* (Santa Monica, CA), Inst. of Electrical and Electronics Engineers, 1981, pp. 119–123.

[14]Junkins, J. L., Rajaram, S., and Baracat, W., "Precision Autonomous Satellite Attitude Control Using Momentum Transfer and Magnetic Torquing," *Journal of the Astronautical Sciences*, Vol. 30, No. 1, 1981, pp. 31–48.

[15]Hunt, R., Su, L. R., and Meyer, G., "Design for Multi-Input Nonlinear Systems," *Differential Geometric Control Theory*, edited by R. Brockett, R. Willman, and H. Sussmann, Birhäuser, Boston, 1983, pp. 268–298.

[16]Isidori, A., Krener, A., Gori-Giorgi, C., and Monaco, S., "Nonlinear Decouping via Feedback: A Differential Geometric Approach," *IEEE Transactions on Automatic Control*, Vol. AC-26, 1981, pp. 331–345.

[17]Isidori, A., *Nonlinear Control Systems*, Springer–Verlag, New York, 1989, Chaps. 1–5.

[18]Nijmeijer, H., and van der Schaft, S. J., *Nonlinear Dynamical Systems*, Springer–Verlag, New York, 1990, Chaps. 2–4.

[19]Slotine, J., and Li, W., *Applied Nonlinear Control*, Prentice–Hall, Englewood Cliffs, NJ, 1991, Chaps. 3–5.

[20]Nam, K., and Arapostathis, A., "A Model Reference Adaptive Control Scheme for Pure-Feedback Nonlinear Systems," *IEEE Transactions on Automatic Control*, Vol. AC-33, Sept. 1988, pp. 803–811.

[21]Sastry, S., and Isidori, A., "Adaptive Control of Linearizable Systems," *IEEE Transactions on Automatic Control*, Vol. AC-34, Nov. 1989, pp. 1123–1131.

[22]Taylor, D. G., Kokotovic, P. V., Marino, R., and Kanellakopoulos, I., "Adaptive Relation of Nonlinear Systems with Unmodeled Dynamics," *IEEE Transactions on Automatic Control*, Vol. AC-34, No. 4, 1989, pp. 405–412.

[23]Marino, R., and Tomei, P., "Global Adaptive Output-Feedback Control of Nonlinear Systems," *Proceedings of the 30th Conference on Decision and Control*, Vol. 2, Inst. of Electrical and Electronics Engineers, 1991, pp. 1077–1081.

[24]Kanellakopoulos, I., Kokotovic, P. V., and Morse, A. S., "Systematic Design of Adaptive Controllers for Feedback Linearizable Systems," *IEEE Transactions on Automatic Control*, Vol. AC-36, Nov. 1991, pp. 1241–1253.

[25]Pomet, J.-B., and Praly, L., "Adaptive Nonlinear Control: An Estimation-Based Algorithm," *New Trends in Nonlinear Control Theory*, edited by J. Descusse, M. Fliess, A. Isidori, and D. Leborgne, Springer–Verlag, New York, 1988.

[26]Campion, G., and Bastin, G., "Indirect Adaptive State Feedback Control of Linearly Parameterized Nonlinear Systems," *International Journal of Adaptive Control and Signal Processing*, Vol. 4, 1990, pp. 345–358.

[27]Han, Y., Sinha, N. K., and Elbestawi, M. A., "Adaptive Tracking in Pure-Feedback Nonlinear Systems," *Proceedings of the 30th Conference on Decision and Control* (Brighton, England, UK), Inst. of Electrical and Electronics Engineers, 1991, pp. 2470–2475.

[28]Teel, A., Kadiyala, R., Kokotovic, P., and Sastry, S., "Indirect Techniques for Adaptive Input-Output Linearization of Nonlinear Systems," *International Journal of Control*, Vol. 4, 1990, pp. 345–358.

[29]Vadali, S. R., and Junkins, J. L., "Spacecraft Large Angle Rotational Maneuvers with Optimal Momentum Transfer," *Journal of the Astronautical Sciences*, Vol. 31, No. 2, 1983, pp. 217–235.

[30]Wie, B., and Barba, P., "Quaternion Feedback for Spacecraft Large Angle Maneuvers," *Journal of Guidance, Control, and Dynamics*, Vol. 8, No. 3, 1985, pp. 360–365.

[31]Creamer, N. G., and Gates, M. L. S., "Attitude Determination and Control of Clementine During Lunar Mapping," *Journal of Guidance, Control, and Dynamics*, Vol. 19, No. 3, 1996, pp. 505–511.

[32]Junkins, J. L., Akella, M. R., and Robinett, R. D., "Nonlinear Adaptive Control of Spacecraft Near-Minimum-Time Maneuvers," AAS Space Flight Mechanics Conf., Huntsville, AL, 1997; also *Journal of the Astronautical Sciences* (to be published).

[33]Tsiotras, P., "New Control Laws for the Attitude Stabilization of Rigid Bodies," *IFAC Symposium on Automatic Control in Aerospace* (Palo Alto, CA), AIAA, Washington, DC, 1994, pp. 316–321.

[34]Sheen, J. J., and Bishop, R. H., "Spacecraft Nonlinear Control," *Journal of the Astronautical Sciences*, Vol. 42, No. 3, 1994, pp. 361–377.

[35]Sheen, J. J., and Bishop, R. H., "Adaptive Nonlinear Control of Spacecraft," *Journal of the Astronautical Sciences*, Vol. 42, No. 4, 1994, pp. 451–472.

[36]Dzielski, J., Bergmann, E., and Paradiso, J., "Approach to Control Moment Gyroscope Steering Using Feedback Linearization," *Journal of Guidance, Control, and Dynamics*, Vol. 14, No. 1, 1991, pp. 96–106.

[37]Singh, S. N., and Iyer, A., "Nonlinear Regulation of Space Station: A Geometric Approach," *Journal of Guidance, Control, and Dynamics*, Vol. 17, No. 2, 1994, pp. 242–249.

[38]Singh, S. N., and Bossart, T. C., "Invertibility of Map, Zero Dynamics and Nonlinear Control of Space Station," *AIAA Guidance, Navigation, and Control Conference*, CP2663, Vol. 1, AIAA, Washington, DC, 1991, pp. 576–584.

[39]Paynter, S. J., and Bishop, R. H., "Indirect Adaptive Nonlinear Attitude Control and Momentum Management of Spacecraft Using Feedback Linearization," AAS Astrodynamics Specialists Conf., Halifax, NS, Canada, Aug. 1995 (Paper 06-418).

[40]Junkins, J. L., Carrington, C. K., and Williams, C. E., "Time Optimal Magnetic Attitude Maneuvers," *Journal of Guidance and Control*, Vol. 4, No. 4, 1981, pp. 363–368.

[41]Junkins, J. L., and Turner, J. D., "Optimal Continuous Torque Attitude Maneuvers," *Journal of Guidance and Control*, Vol. 3, No. 3, 1980, pp. 210–217.

[42]Carrington, C., and Junkins, J. L., "Optimal Nonlinear Feedback Control for Spacecraft Attitude Maneuvers," *Journal of Guidance, Control, and Dynamics*, Vol. 9, No. 1, 1986, pp. 99–107.

[43]Junkins, J. L., Rahman, Z. H., and Bang, H., "Near-Minimum-Time Maneuvers of Distributed Parameter Systems: Analytical and Experimental Results," *Journal of Guidance, Control, and Dynamics*, Vol. 14, No. 2, 1991, pp. 406–415.

[44]Bang, H., Junkins, J. L., and Fleming, P., "Lyapunov Optimal Control Laws for Flexible Structure Maneuver and Vibration Control," *Journal of the Astronautical Sciences*, Vol. 41, No. 1, 1993, pp. 91–118.

[45]Mukherjee, R., and Junkins, J. L., "An Invariant Set Analysis of the Hub-Appendage Problem," *Journal of Guidance, Control, and Dynamics*, Vol. 16, No. 6, 1993, pp. 1191–1193.

[46]Bell, M., and Junkins, J. L., "Near Minimum-Time Three Dimensional Maneuvers of Rigid and Flexible Spacecraft," *Journal of the Astronautical Sciences*, Vol. 42, No. 4, 1994, pp. 421–438.

[47]Robinett, R. D., Parker, G. P., Schaub, H., and Junkins, J. L., "Lyapunov Optimal Saturated Control for Nonlinear Systems," *Journal of Guidance, Control, and Dynamics*, Vol. 20, No. 6, 1997, pp. 1083–1088.

[48]Junkins, J. L., Akella, M. R., and Alfriend, K. T., " Non-Gaussian Error Propagation in Orbital Mechanics," *Journal of the Astronautical Sciences* (to be published).

[49]Junkins, J. L., *Optimal Estimation of Dynamical Systems*, Sijhoff and Noordhoff, Alphen aan den Rijn, The Netherlands, 1977, Chaps. 1–6.

[50]Shuster, M., "A Survey of Attitude Representations," *Journal of the Astronautical Sciences*, Vol. 41, No. 4, 1993, pp. 439–518.

[51]Schaub, H., and Junkins, J. L., "Stereographic Orientation Parameters for Attitude Dynamics: A Generalization of the Rodrigues Parameters," *Journal of the Astronautical Sciences*, Vol. 44, No. 1, 1996, pp. 1–20.

[52]Tsiotras, P., Junkins, J. L., and Schaub, H., "Higher Order Cayley Transforms with Applications to Attitude Representations," AAS Astrodynamics Specialist Conf., San Diego, CA, 1996 (Paper AAS 96-3628).

[53]Oshman, Y., and Bar-Itzhack, I. Y., "Eigenfactor Solution of the Matrix Riccati Equation—A Continuous Square Root Algorithm," *IEEE Transactions on Automatic Control*, Vol. AC-30, No. 10, 1985, pp. 971–978.

[54]Junkins, J. L., and Schaub, H., "Orthogonal Square Root Eigenfactor Parameterization of Mass Matrices," *Journal of Guidance, Control, and Dynamics*, Vol. 20, No. 6, 1997, pp. 1118–1124.

[55]Schaub, H., Tsiotras, P., and Junkins, J. L., "Principal Rotation Representations of Proper $N \times N$ Orthogonal Matrices," *International Journal of Engineering Science*, Vol. 33, No. 15, 1995, pp. 2277–2295.

[56]Kim, Y., Lee, S., and Junkins, J. L., "Eigenvector Derivatives for Mechanical Second-Order Systems," *Journal of Guidance, Control, and Dynamics*, Vol. 18, No. 4, 1995, pp. 899–906.

[57]Lin, R. M., and Lim, M. K., "Eigenvector Derivatives of Structures with Rigid Body Modes," *AIAA Journal*, Vol. 34, No. 5, 1996, pp. 1083–1085.

[58]Dailey, R. L., "Eigenvector Derivatives with Repeated Eigenvalues," *AIAA Journal*, Vol. 27, No. 4, 1989, pp. 486–491.

[59]Mills-Curran, W. C., "Calculation of Eigenvector Derivatives for Structures with Repeated Eigenvalues," *AIAA Journal*, Vol. 26, No. 7, 1988, pp. 867–871.

[60]Zhang, D.-W., and Wei, F.-S., "Computation of Eigenvector Derivatives with Repeated Eigenvalues Using a Complete Modal Space," *AIAA Journal*, Vol. 33, No. 9, 1995, pp. 1749–1753.

[61]Zhang, Y.-Q., and Wang, W.-L., "Eigenvector Derivatives of Generalized Nondefective Eigenproblems with Repeated Eigenvalues," *Journal of Engineering for Gas Turbines and Power*, Vol. 117, Jan. 1995, pp. 207–212.

[62]Junkins, J. L., and Schaub, H., "Eigenfactor Parameterization of the Mass Matrix," AAS Space Flight Mechanics Conf., Huntsville, AL, 1997; also *Journal of the Astronautical Sciences* (to be published).

[63]Schaub, H., Junkins, J. L., and Robinett, R. D., "New Penalty Functions and Optimal Control Formulation for Spacecraft Attitude Control Problems," *Journal of Guidance, Control, and Dynamics*, Vol. 20, No. 3, 1997, pp. 428–434.

[64]Junkins, J. L., White, C. C., and Turner, J. D., "Star Pattern Recognition for Real Time Attitude Determination," *Journal of the Astronautical Sciences*, Vol. 25, No. 3, 1977, pp. 251–270.

[65]Junkins, J. L., and Strikwerda, T., "Autonomous Star Sensing and Attitude Estimation," *Advances in the Astronautical Sciences*, edited by P. Pergo, B. Kaufman, L. Friedman, and R. Battin, Vol. 39, Univelt, San Diego, 1991, pp. 155–184.

[66]Strikwerda, T., "Near Earth Asteroid Rendezvous Guidance and Control System," SAE Aerospace Control and Guidance Systems Meeting (Nashville, TN), Society of Automotive Engineers, Warrendale, PA, Oct. 1996.

[67]DeLaHunt, P., and Creamer, N. G., "Clementine Attitude Determination and Control System," *Journal of Spacecraft and Rockets*, Vol. 32, No. 6, 1995, pp. 1054–1059.

[68]Nozette, S., Lichtenberg, C. L., Spudis, P., Bonner, R., Ort, W., Malaret, E., Robinson, M., and Shoemaker, E. M., "The Clementine Bistatic Radar Experiment," *Science*, Vol. 274, No. 5292, 1996, pp. 1495–1498.